QUANTITATIVE FINANCE
RESEARCH CENTRE

UNIVERSITY OF
TECHNOLOGY SYDNEY

QUANTITATIVE FINANCE RESEARCH CENTRE

Research Paper 365 November 2015

Volatility Clustering: A Nonlinear Theoretical Approach

Xue-Zhong He, Kai Li and Chuncheng Wang

ISSN 1441-8010 www.qfrc.uts.edu.au

VOLATILITY CLUSTERING: A NONLINEAR THEORETICAL APPROACH

XUE-ZHONG HE*,†, KAI LI* AND CHUNCHENG WANG**

*University of Technology Sydney

Business School, Finance Discipline Group

PO Box 123, Broadway, NSW 2007, Australia

**Harbin Institute of Technology

Department of Mathematics

Harbin 150001, Heilongjiang, China

tony.he1@uts.edu.au

kai.li@uts.edu.au

wangchuncheng@hit.edu.cn

Date: November 3, 2015.

Acknowledgement: Financial support from the Australian Research Council (ARC) under Discovery Grant (DP130103210) is gratefully acknowledged. The usual caveats apply.

† *Corresponding author.*

ABSTRACT. This paper verifies the endogenous mechanism and economic intuition on volatility clustering using the coexistence of two locally stable attractors proposed by Gaunersdorfer, Hommes and Wagener (2008). By considering a simple asset pricing model with two types of boundedly rational traders, fundamentalists and trend followers, and noise traders, we provide conditions on the coexistence of locally stable steady state and invariant cycle of the underlying nonlinear deterministic financial market model and show numerically that the interaction of the coexistence of the deterministic dynamics and noise processes can endogenously generate volatility clustering and long range dependence in volatility observed in financial markets. Economically, volatility clustering occurs when neither the fundamental nor trend following traders dominate the market and when traders switch more often between the two strategies.

Key words: Volatility clustering, fundamentalists and trend followers, bounded rationality, stability, coexisting attractors.

JEL Classification: D84, E32, G12

1. Introduction

Volatility clustering, one of the most important stylized facts in financial markets, refers to the observation that large changes in price tend to be followed by large changes and small changes tend to be followed by small changes. In other words, asset price fluctuations display irregular interchanging between high volatility and low volatility episodes. Since it was first observed by Mandelbrot (1963) in commodity prices, volatility clustering has been widely observed and documented in stocks, market indices and exchange rates. Despite the extensive development of various statistical models following the ARCH and GARCH models pioneered by Engle (1982) and Bollerslev (1986), these models offer very limited economical explanation of the mechanism in generating the volatility clustering.

Recent development of asset pricing models based on boundedly rational traders with heterogeneous beliefs has proposed a number of mechanism explanations. In particular, Gaunersdorfer et al. (2008) propose an endogenous mechanism and economic intuition based on the coexistence of a stable steady state and a stable limit cycle. In this paper, we consider a simple asset pricing model with two types of boundedly rational traders, fundamentalists and trend followers, and noise traders. By applying normal form analysis and the center manifold theory on the underlying nonlinear deterministic model, we provide conditions on the coexistence of a stable steady state and a stable closed invariant cycle. When buffered with noises, the stochastic model can endogenously generate volatility clustering and long range dependence in volatility observed in financial markets. Economically, with strong trading activities of either the fundamental investors or the trend followers, market price fluctuates around either the fundamental value with low volatility or a cyclical price movement with high volatility depending on market conditions. With the fundamental noise and noise traders, this triggers an irregular shifting between two volatility regimes and therefore leads to volatility clustering. In particular, the effect becomes more significant when traders switch their strategies more often. We therefore verify the endogenous mechanism on volatility clustering proposed by Gaunersdorfer et al. (2008) and provide an economic explanation on the volatility clustering.

Gaunersdorfer et al. (2008) propose two generic mechanisms to explain the volatility clustering: one is the coexistence of a stable steady state and a stable limit cycle and the other is the intermittency and associated bifurcation routes to strange attractors. They provide very nice economic intuitions on how the mechanisms could be used to explain the volatility clustering and why these phenomena arise in nonlinear evolutionary financial systems. The main idea behind the first proposed mechanism of Gaunersdorfer et al. (2008) is that a locally stable steady state and a locally stable closed invariant circle coexist in a nonlinear financial market system. When the price is attracted by the stable steady state, that is when the fundamentalists are more active in the market, the price is stable and the corresponding return is less volatile. However when the trend followers exhibit strong trading activity, the market price is attracted by the stable circle, leading to large price fluctuation and high volatility in returns. Buffeted with noises in the market, the price process irregularly switches between the two stable regions from time to time. As a result, the irregular interchanging between the two attractors triggered by large random shocks leads the return process to exhibit volatility clustering. Mathematically, Gaunersdorfer et al. (2008) demonstrate the coexistence through a Chenciner bifurcation, a codimension-two bifurcation in which two parameters vary simultaneously. Near the Chenciner bifurcation point, there exists an open region, called "volatility clustering region", in a two-dimensional parameter subspace in which a stable steady state and a stable limit cycle coexist. Due to the complexity of the normal form analysis of codimension-two bifurcation, they identify the volatility clustering region numerically and indicate the potential of the mechanism in generating volatility clustering. The proposed mechanism has also been used to explain path dependent coordination of expectations in asset pricing experiments. In the learning-to-forecast laboratory experiments, Hommes, Sonnemans, Tuinstra and van de Velden (2005) find three different types of aggregate asset price behavior: monotonic convergence to the stable fundamental steady state, dampened price oscillations and permanent price oscillations. Motivated by the mechanism of Gaunersdorfer et al. (2008), Agliari, Hommes and Pecora (2015) develop a simple behavior model with switching and

explain individual as well as the three different types of aggregate behavior in the experiments through the coexistence mechanism.

In this paper, we obtain analytical conditions on the coexistence of a stable steady state and a stable closed invariant cycle and provide a systematic way to identify "volatility clustering interval" by examining the stability of a Neimark-Sacker bifurcation through the change of one parameter.[1] More explicitly, we first apply the stability and bifurcation analysis to examine the local stability of the steady state with respect to a Neimark-Sacker bifurcation parameter. We then investigate the direction and the stability of the bifurcated closed invariant cycle by applying the normal form method and the center manifold theory. The coexistence is then jointly determined by the conditions when the steady state is locally stable and the bifurcated cycle is backward and unstable. In this case, the bifurcated unstable cycle can be extended backward with respect to the bifurcation parameter until a threshold value and then the extended cycle becomes forward and stable. Therefore, the stable steady state coexists with the stable 'forward extended' cycle, in between the 'backward extended' cycle is unstable. Correspondingly, there exists an interval for the bifurcation parameter in which the two locally stable attractors coexist. This implies that, even when the fundamental steady state is locally stable, prices need not converge to the fundamental value, but may settle down to a stable limit cycle, depending on the initial conditions. Based on the conditions on the coexistence, we further demonstrate numerically that the stochastic model is able to generate various stylized facts, including non-normality in asset returns, volatility clustering, and long range dependence in volatility observed in financial markets. Therefore we

[1]Gaunersdorfer et al. (2008) illustrate the coexistence through Chenciner bifurcation, which requires Hopf bifurcation plus the condition on the first Lyapunov coefficient $a(0) = 0$. The advantage of our method over the analysis merely based on Chenciner is that we can detect systematically the coexistence interval. This advantage is based on the analysis of both bifurcation direction and bifurcation stability, which provide results with respect to one parameter. In general both the bifurcation direction and stability are determined by different conditions, however for our model, they are completely determined by a(0) only (due to $\rho'(\gamma^{**}) > 0$; see Theorem B.3). This simplifies our analysis by focusing on the first Lyapunov coefficient.

provide theoretical foundation and numerically supporting evidence on the proposed mechanism of Gaunersdorfer et al. (2008).

This paper contributes to the heterogeneous agent models (HAMs) literature by providing better understanding of the global dynamics of the underlying nonlinear deterministic financial market model, the interaction between deterministic global dynamics and noises, and therefore complexity of financial market behavior. Following the seminal work of Brock and Hommes (1997, 1998), various HAMs have been developed to incorporate adaptation, evolution, heterogeneity, and even learning with both Walrasian and market maker market clearing scenarios.[2] Those models have successfully explained various market behavior (such as market booms and crashes, long deviations of the market price from the fundamental price), the stylized facts (such as skewness, kurtosis, volatility clustering and fat tails of returns), and power laws behavior, including the long range dependence in return volatility observed in financial markets.[3] Given the complexity of nonlinear financial market systems, most work on HAMs is computationally oriented based on the local stability and bifurcation analysis. The globally nonlinear properties are seldom analyzed.[4] In fact, the coexistence of two locally stable attractors involves the stability analysis of the bifurcated cycle, which is beyond the local analysis on constant steady state. In this paper we apply the normal form method and the center manifold theory to conduct a global analysis on the coexistence phenomenon of the HAM developed in Dieci, Foroni, Gardini and He (2006). In this model, apart from noise traders, there are two types of traders in a financial market: fundamentalists, who believe that prices will move in the direction of the fundamental value, and trend followers

[2]See, for example, the market maker scenario in Farmer and Joshi (2002) and Chiarella and He (2003); the impact of heterogeneous risk aversion and learning in Chiarella and He (2002); the dynamics of moving averages in Chiarella, He and Hommes (2006); and complex price dynamics within a multi-asset market framework in Westerhoff (2004).

[3]We refer readers to Hommes (2006), LeBaron (2006), Chiarella, Dieci and He (2009), and Lux (2009) for surveys of the recent development in this literature.

[4]He, Li, Wei and Zheng (2009) is one of the few exceptions. In addition to the local stability analysis, He et al. (2009) analytically examine the bifurcation properties, including the direction of the bifurcation and the stability of the bifurcated cycle, and the global extension of the bifurcated cycle.

or chartists, who extrapolate the latest observed price change. The fractions of the two different types of the traders change over time according to the evolutionary fitness of the two strategies, as measured by the realized profits.

Apart from Gaunersdorfer et al. (2008) (and Gaunersdorfer and Hommes (2007)), there are other two different mechanisms in generating the volatility clustering that have been proposed: the herding mechanism in Alfarano, Lux and Wagner (2005) and the stability switching near the bifurcation boundary in He and Li (2007). By considering an extremely parsimonious stochastic herding model with fundamentalists (who trade on observed mispricing) and noise traders (who follow the mood of the market), Alfarano et al. (2005) show that price changes are generated by either exogenous inflow of new information about fundamentals or endogenous changes in demand and supply via the herding mechanism. The model is able to produce return time series whose distributional and temporal characteristics are astonishingly close to the empirical findings, including the volatility clustering and long range dependence in volatility. The generating mechanism is due to a bi-modal limiting distribution for the fraction of noise traders in the optimistic and pessimistic groups of individuals and the stochastic nature of the process, which leads to recurrent switches from one majority to another. By considering a simple market fraction asset pricing model with fundamental and trend following investors, He and Li (2007) show that, even when the fundamental steady state is locally stable, for parameter values near the bifurcation boundary, the risk-adjusted trend chasing and the interplay of the noises and the underlying deterministic dynamics can generate volatility clustering and power-law distributed fluctuations. Intuitively, with the risk-adjusted trend chasing behaviour from the trend followers and stabilizing role of the fundamentalists, the price dynamics do not explode when the fundamental steady state becomes unstable. Buffered with fundamental and market noises, the price dynamics interchange between stable and unstable fundamental steady state. This mechanism shares a similar mechanism to the coexistence of two locally stable attractors in a much simpler and very different way. The statistic analysis based on model calibration and Monte Carlo simulations in He and Li (2007, 2015*b*) provides further evidence on the mechanism. Different from these two mechanisms, the

analysis of this paper provides a better understanding and further insight into the mechanism from a global dynamics point of view.

The paper is organized as follows. We first outline a stochastic HAM of asset pricing developed in Dieci et al. (2006) in Section 2. In Section 3, we apply the stability and bifurcation theory, together with the normal form analysis and the center manifold theory, to examine the coexistence of a local stable fundamental price and a locally stable closed cycle around the fundamental price. Section 4 conducts analysis on the stochastic model numerically. It explores the joint impact of the coexistence effect of the deterministic dynamics and noises on generating various market behavior and the stylized facts, including volatility clustering and long range dependence. Section 5 concludes. All the proofs are included in the appendices.

2. The Model

The model introduced here has been developed in Dieci et al. (2006) and then extended in He and Li (2015*c*). The model of Dieci et al. (2006) is a standard discounted asset pricing model with two types of heterogeneous agents, the fundamentalists and trend followers, and population evolution. To provide an economic intuition of the market noise, He and Li (2015*c*) extend the model to include noise traders explicitly and show that the resulting model is in fact the same as the model in Dieci et al. (2006). For completeness we outline the model and refer readers to Dieci et al. (2006) and He and Li (2015*c*) for the details.

Consider an economy with one risky asset and one risk free asset. It is assumed that the risk free asset is perfectly elastically supplied at gross return of $R = 1+r/K$, where r is the constant risk-free rate per annum and K is the trading frequency measured in units of a year.[5] Let p_t and D_t be the (ex dividend) price and dividend per share of the risky asset at time t, respectively.

There are three types of traders (or investors/agents), fundamental traders (or fundamentalists), trend followers (or chartists) and noise traders, denoted by type

[5]Typically, $K = 1$, 12; 52 and 250 representing trading periods of year, month, week and day, respectively. To calibrate the stylized facts observed from daily price movement in financial market, we select $K = 250$ in our discussion.

$1, 2$ and 3 traders respectively. Let $Q_{i,t}(i = 1, 2, 3)$ be their market fractions at time t, respectively. We assume that there is a fixed fraction of noise traders, denoted by n_3. Among $1 - n_3$, the market fractions of the fundamentalists and trend followers have fixed and time-varying components. Denote by n_1 and n_2 the fixed proportions of fundamentalists and trend followers among $1 - n_3$, respectively. Then $(1-n_3)(n_1+n_2)$ represents the proportion of traders who do not change their strategies over time, while $(1 - n_3)[1 - (n_1 + n_2)]$ is the proportion of traders who may switch between the two types. Among the switching traders, we denote $n_{1,t}$ and $n_{2,t} = 1 - n_{1,t}$ the proportions of fundamentalists and trend followers at time t, respectively. It follows that the market fractions $(Q_{1,t}, Q_{2,t}, Q_{3,t})$ at time t are expressed by

$$Q_{1,t} = (1-n_3)[n_1+(1-n_1-n_2)n_{1,t}], \quad Q_{2,t} = (1-n_3)[n_2+(1-n_1-n_2)n_{2,t}], \quad Q_{3,t} = n_3.$$

Denote $n_0 = n_1 + n_2, m_0 = (n_1 - n_2)/n_0$ and $m_t = n_{1,t} - n_{2,t}$. Then the market fractions at time t can be rewritten as

$$\begin{cases} Q_{1,t} &= \frac{1}{2}(1 - n_3)\left[n_0\left(1 + m_0\right) + \left(1 - n_0\right)\left(1 + m_t\right)\right], \\ Q_{2,t} &= \frac{1}{2}(1 - n_3)\left[n_0\left(1 - m_0\right) + \left(1 - n_0\right)\left(1 - m_t\right)\right], \\ Q_{3,t} &= n_3 \end{cases} \tag{2.1}$$

For a typical investor-h, his wealth $W_{h,t+1}$ at $t + 1$ is given by

$$W_{h,t+1} = RW_{h,t} + (p_{t+1} + D_{t+1} - Rp_t)z_{h,t}, \tag{2.2}$$

where $z_{h,t}$ is the number of shares of the risky asset purchased by investor-h at t. Let $E_{h,t}$ and $V_{h,t}$ be the beliefs of type h traders about the conditional expectation and variance at $t + 1$ based on their information at time t. Denote by $R_{t+1}(= p_{t+1} + D_{t+1} - Rp_t)$ the excess capital gain on the risky asset at $t + 1$. Assume that type h traders have constant absolute risk aversion (CARA) utility functions with a risk aversion coefficient a_h, that is $U_h(W) = -e^{-a_h W}$. Then, under the standard conditional normality assumption, their optimal demands on the risky asset $z_{h,t}$ are determined by

$$z_{h,t} = \frac{E_{h,t}(R_{t+1})}{a_h V_{h,t}(R_{t+1})}. \tag{2.3}$$

Assume the demand of the noise traders is given by $\tilde{\xi}_t \sim N(0, \sigma_\xi^2)$, which is an i.i.d. random disturbance. With zero supply of outside shares, the population weighted average excess demand $\tilde{Z}_{e,t}$ at time t is given by

$$\tilde{Z}_{e,t} \equiv Q_{1,t}\, z_{1,t} + Q_{2,t}\, z_{2,t} + n_3 \tilde{\xi}_t.$$

Following Chiarella and He (2003), the market price in each trading period is determined by a market maker who adjusts the price as a function of the excess demand. The market maker takes a long position when $\tilde{Z}_{e,t} < 0$ and a short position when $\tilde{Z}_{e,t} > 0$. The market price is adjusted according to

$$p_{t+1} = p_t + \lambda \tilde{Z}_{e,t}, \tag{2.4}$$

where λ denotes the speed of price adjustment of the market maker. Denote $\mu = (1 - n_3)\lambda$ and $\sigma_\delta = \lambda n_3 \sigma_\xi$. Then equation (2.4) becomes

$$p_{t+1} = p_t + \mu Z_{e,t} + \tilde{\delta}_t, \tag{2.5}$$

where $Z_{e,t} = q_{1,t}\, z_{1,t} + q_{2,t}\, z_{2,t}$ and $\tilde{\delta}_t \sim N(0, \sigma_\delta^2)$ with

$$\begin{cases} q_{1,t} = Q_{1,t}/(1 - n_3) = [n_0(1 + m_0) + (1 - n_0)(1 + m_t)]/2, \\ q_{2,t} = Q_{2,t}/(1 - n_3) = [n_0(1 - m_0) + (1 - n_0)(1 - m_t)]/2. \end{cases} \tag{2.6}$$

The price equation (2.5) is exactly the same model developed in Dieci et al. (2006).

We now describe briefly the heterogeneous beliefs of the fundamentalists and trend followers and the adaptive switching mechanism, as in Dieci et al. (2006). Denote by $F_t = \{p_t, p_{t-1}, \cdots; D_t, D_{t-1}, \cdots\}$ the common information set formed at time t. Apart from the common information set, the fundamentalists are assumed to have superior information on the fundamental value, p_t^*, of the risky asset which is introduced as an exogenous news arrival process. More precisely, the relative return $p_{t+1}^*/p_t^* - 1$ of the fundamental value is assumed to follow a normal distribution,

$$p_{t+1}^* = p_t^*[1 + \sigma_\epsilon \tilde{\epsilon}_t], \qquad \tilde{\epsilon}_t \sim \mathcal{N}(0, 1), \qquad \sigma_\epsilon \geq 0, \qquad p_0^* = \bar{p} > 0, \tag{2.7}$$

where $\tilde{\epsilon}_t$ is independent of the noisy demand process $\tilde{\delta}_t$ and $\bar{p}$ is a constant to be specified. Fundamental traders believe that the stock price may be driven away from the fundamental price in the short run, but it will eventually return to the

fundamental value in the long-run. Thus the conditional mean and variance of the price for the fundamental traders are assumed to follow

$$E_{1,t}\left(p_{t+1}\right) = p_t + (1-\alpha)(E_t[p^*_{t+1}] - p_t), \qquad V_{1,t}\left(p_{t+1}\right) = \sigma_1^2, \tag{2.8}$$

where σ_1^2 is a constant variance on the price. The speed of adjustment towards the fundamental price is represented by $(1-\alpha)$, where $0 < \alpha < 1$. An increase in α may thus indicate less confidence on the convergence to the fundamental price, leading to a slower adjustment.

Unlike the fundamental traders, trend followers are assumed to extrapolate the latest observed price deviation from a long run sample mean price. More precisely, their conditional mean and variance are assumed to follow

$$E_{2,t}\left(p_{t+1}\right) = p_t + \gamma\left(p_t - u_t\right), \qquad V_{2,t}\left(p_{t+1}\right) = \sigma_1^2 + b_2 v_t, \tag{2.9}$$

where $\gamma \geq 0$ measures the extrapolation from the trend, u_t and v_t are sample mean and variance, respectively, which follow

$$u_t = \delta u_{t-1} + (1-\delta)\, p_t, \qquad v_t = \delta v_{t-1} + \delta\,(1-\delta)\left(p_t - u_{t-1}\right)^2,$$

representing limiting processes of geometric decay processes when the memory lag tends to infinity.[6] Here $b_2 \geq 0$ measures the sensitivity to the sample variance and $\delta \in (0,1)$ measures the geometric decay rate. Note that a constant variance is assumed for the fundamentalists who believe the mean reverting of the market price to the fundamental price; while a time-varying component of the variance for the trend followers reflects the extra risk they take by chasing the trend.

We now specify how traders compute the conditional variance of the dividend D_{t+1} and of the excess return R_{t+1} over the trading period. For simplicity we assume that traders share homogeneous belief about the dividend process and that the trading period dividend D_t is i.i.d. and normally distributed with mean $\bar{D}$ and variance σ_D^2. Denote by $\bar{p} = \bar{D}/(R-1) = (K/r)\bar{D}$ the long-run fundamental price. The common estimate of the variance of the dividend (σ_D^2) is assumed to be proportional to the variance of the fundamental price, with no correlation between price and dividend.

[6]With a geometric decaying probability distribution $(1-\delta)\{1, \delta, \delta^2, \delta^3, \cdots\}$ over the historical prices $\{p_t, p_{t-1}, p_{t-2}, p_{t-3}, \cdots, \}$, u_t and v_t are the corresponding sample mean and variance.

It follows that traders' conditional variances of the excess return can be estimated[7] as $V_{1,t}\left(R_{t+1}\right) = \left(1+r^2\right)\sigma_1^2$ and $V_{2,t}\left(R_{t+1}\right) = \sigma_1^2\left(1+r^2+bv_t\right)$, where $b = b_2/\sigma_1^2$. Using (2.8) and (2.9), it turns out that the optimal demands of the fundamentalists and trend followers are determined by, respectively,

$$z_{1,t} = \frac{(\alpha-1)\left(p_t - p_{t+1}^*\right) - (R-1)\left(p_t - \bar{p}\right)}{a_1\left(1+r^2\right)\sigma_1^2}, \quad z_{2,t} = \frac{\gamma\left(p_t - u_t\right) - (R-1)\left(p_t - \bar{p}\right)}{a_2\sigma_1^2\left(1+r^2+bv_t\right)}. \tag{2.10}$$

Denote by $\pi_{h,t+1}$ the realized profit, or excess return, between t and $t+1$ by type h traders, $\pi_{h,t+1} = z_{h,t}(p_{t+1} + D_{t+1} - Rp_t) = W_{h,t+1} - RW_{h,t}$ for $h = 1, 2$. Following Brock and Hommes (1997, 1998), the proportion of "switching" traders at time $t+1$ is determined by

$$n_{h,t+1} = \frac{\exp\left[\beta\left(\pi_{h,t+1} - C_h\right)\right]}{\sum_{i=1}^{2}\exp\left[\beta\left(\pi_{i,t+1} - C_i\right)\right]}, \qquad h = 1, 2,$$

where $C_h \geq 0$ is a fixed cost associated with strategy h, parameter β is the *intensity of choice* measuring the switching sensitivity of the population of adaptively rational traders to the better profitable strategy. It follows from $m_{t+1} = n_{1,t+1} - n_{2,t+1}$ that

$$m_{t+1} = \tanh\left\{\frac{\beta}{2}[(\pi_{1,t+1} - \pi_{2,t+1}) - (C_1 - C_2)]\right\}. \tag{2.11}$$

[7]The long-run fundamental value is given by $\bar{p} = (K\bar{D})/r$, where $K\bar{D}$ is the average annual dividend. Let $\sigma\bar{p}$ be the annual volatility of the price p, where σ represents the annual volatility of 1 dollar invested in the risky asset. Under independent price increments, the trading period variance of the price can be estimated as $\sigma_1^2 = \left(\bar{p}\sigma\right)^2/K$. Denote by D_A and $\sigma_{D_A}^2$ the annual dividend and its variance respectively and assume an approximate relationship $D_A = rp$ between annual dividend and price. Then one gets $\sigma_{D_A}^2 = r^2(\sigma\bar{p})^2$ and therefore $\sigma_D^2 = \sigma_{D_A}^2/K = r^2(\sigma\bar{p})^2/K = r^2\sigma_1^2$. Assuming zero correlation between price and dividend, then $V_{1,t}\left(R_{t+1}\right) = \left(1+r^2\right)\sigma_1^2$ and $V_{2,t}\left(R_{t+1}\right) = \sigma_1^2(1+r^2) + b_2v_t$.

Together with (2.6) the market fractions and asset price dynamics are determined by the following random discrete-time dynamical system

$$\begin{cases} p_{t+1} = p_t + \mu(q_{1,t}\, z_{1,t} + q_{2,t}\, z_{2,t}) + \widetilde{\delta}_t, \\ u_t = \delta u_{t-1} + (1-\delta)\, p_t, \\ v_t = \delta v_{t-1} + \delta\,(1-\delta)\,(p_t - u_{t-1})^2\,, \\ m_t = \tanh\left\{\dfrac{\beta}{2}\left[(z_{1,t-1} - z_{2,t-1})\,(p_t + D_t - Rp_{t-1}) - (C_1 - C_2)\right]\right\}, \\ p^*_{t+1} = p^*_t[1 + \sigma_\epsilon \tilde{\epsilon}_t], \end{cases} \tag{2.12}$$

where $z_{1,t}$ and $z_{2,t}$ are given by (2.10). In the following sections, we first conduct a global analysis of the underlying deterministic model to examine the coexistence of a locally stable steady state and a locally stable limit cycle.

3. Coexistence of the Nonlinear Deterministic Model

In order to understand the interaction of the deterministic dynamics and the noise processes, we first study the dynamics of the corresponding deterministic model in this section. Without market noise and fundamental noise, that is, $\widetilde{\delta}_t = 0$ and $p^*_t = \bar{p}$, the stochastic system (2.12) reduces to a deterministic model

$$\begin{cases} p_{t+1} = p_t + \dfrac{\mu}{2}\Big(\left[n_0\,(1+m_0) + (1-n_0)\,(1+m_t)\right]\, z_{1,t} \\ \qquad\qquad + \left[n_0\,(1-m_0) + (1-n_0)\,(1-m_t)\right]\, z_{2,t}\Big), \\ u_t = \delta u_{t-1} + (1-\delta)\, p_t, \\ v_t = \delta v_{t-1} + \delta\,(1-\delta)\,(p_t - u_{t-1})^2\,, \\ m_t = \tanh\left\{\dfrac{\beta}{2}\left[(z_{1,t-1} - z_{2,t-1})\left(p_t + \bar{D} - Rp_{t-1}\right) - (C_1 - C_2)\right]\right\}, \end{cases} \tag{3.1}$$

where

$$z_{1,t} = \frac{(\alpha - R)\,(p_t - \bar{p})}{a_1\,(1+r^2)\,\sigma_1^2}, \qquad z_{2,t} = \frac{\gamma\,(p_t - u_t) - (R-1)\,(p_t - \bar{p})}{a_2\sigma_1^2\,(1 + r^2 + bv_t)}. \tag{3.2}$$

3.1. **No-switching Model.** To understand the impact of the evolution learning on the price dynamics, we first study a special case without population evolution (with $n_o = 1$) by fixing market fractions $q_{1,t}, q_{2,t}$ as constants q_1, q_2. Consequently, system

(3.1) reduces to

$$\begin{cases} p_{t+1} = p_t + \dfrac{\mu}{2}(q_1\, z_{1,t} + q_2\, z_{2,t}), \\ u_t = \delta u_{t-1} + (1-\delta)\, p_t, \\ v_t = \delta v_{t-1} + \delta\,(1-\delta)\,(p_t - u_{t-1})^2\,. \end{cases} \tag{3.3}$$

A stability and bifurcation analysis of system (3.3) with respect to the parameter γ leads to the following result.

Theorem 3.1. *Denote* $\rho = \frac{a_2}{a_1}, Q = 2a_2\sigma_1^2(1+r^2)$,

$$K = \frac{\mu}{Q}[q_1\rho(\alpha - R) + q_2(1-R)](< 0)$$

and

$$\gamma^* = (R-1) + \frac{Q(1-\delta)}{\delta\mu q_2} + \frac{\rho q_1(R-\alpha)}{q_2}. \tag{3.4}$$

(i) *The deterministic system* (3.3) *has a unique fundamental steady state* $(p, u, v) = (\bar{p}, \bar{p}, 0)$.

(ii) *Assume* $-2 < K < 0$. *Then the fundamental steady state* $(\bar{p}, \bar{p}, 0)$ *is locally asymptotically stable for* $\gamma \in (0, \gamma^*)$, *and it undergoes a Neimark-Sacker bifurcation at* $\gamma = \gamma^*$, *that is, there is an invariant cycle near the fundamental steady state.*

(iii) *Moreover, the bifurcated invariant cycle is forward and stable when* $a_1(0) < 0$ *and backward and unstable when* $a_1(0) > 0$, *here the first Lyapunov coefficient* $a_1(0)$ *is defined by* (A.10) *in Appendix A.*

Proof. See Appendix A. □

Theorem 3.1 implies that the fundamental price $\bar{p}$ is locally stable when the activity of the trend followers, measured by γ, is not strong (so that $\gamma < \gamma^*$). Note that γ^* increases as q_1 or ρ increases, or as q_2, δ, α or μ decreases. Intuitively, when the fundamental traders dominate the market, characterized by their high market fraction q_1, high speed of price adjustment $1-\alpha$, and less risk aversion a_1, the fundamental price is stabilized. When the trend followers dominate the market, characterized by their high market fraction q_2, strong extrapolation γ, high weight on the past price trend δ, and less risk aversion a_2, the fundamental price is destabilized. Also, an increase in the price adjustment μ from the market maker always destabilizes the

fundamental price. These results have been explored in Dieci et al. (2006) and He and Li (2007). However, what is new in Theorem 3.1 is part (iii) on the dynamics of the bifurcation based on the normal form analysis and center manifold theory.

On the dynamics, near the bifurcation point $\gamma = \gamma^*$, there exists an invariant cycle around the fundamental steady state, which can be either stable or unstable. From Theorem 3.1 (iii), the stability of the bifurcated invariant cycle depends crucially on the sign of $a_1(0)$, the first Lyapunov coefficient. When $a_1(0) < 0$, the fundamental steady state becomes unstable as γ increases and passes the bifurcation value γ^* and then the solution trajectory of the system converges to a locally stable attractor characterized by the bifurcated invariant cycle. In this case, the bifurcation does not lead to a coexistence of two locally stable attractors. However, when $a_1(0) > 0$, the bifurcation becomes backward and unstable, meaning that the fundamental steady state is still locally stable as γ passes the bifurcation value γ^*; however an invariant cycle is bifurcated from the fundamental steady state as γ decreases from the bifurcation value γ^* and the invariant cycle is unstable. For the no-switching model (3.3), Fig. 3.1 illustrates the first Lyapunov coefficient. Different from the population evolution model (3.1) to be discussed later, Fig. 3.1 shows that $a_1(0)$ is always negative when the market fraction of the fundamental traders q_1 varies from zero to one. This implies that (for the given set of parameters), there is no coexistence of the stable fundamental steady state and a stable invariant cycle for system (3.3). Note that however this does not imply that the corresponding stochastic system for (3.3) is not able to generate volatility clustering. In fact, He and Li (2007) observe volatility clustering generated from this model by choosing a set of parameters close to the bifurcation boundary. Buffered with the fundamental and market noises, the price irregularly switches between the stable region and unstable region, resulting in volatility clustering. This mechanism on the volatility clustering conducted by Monte Carlo simulation and model calibration is different from the analytical mechanism discussed in this paper.

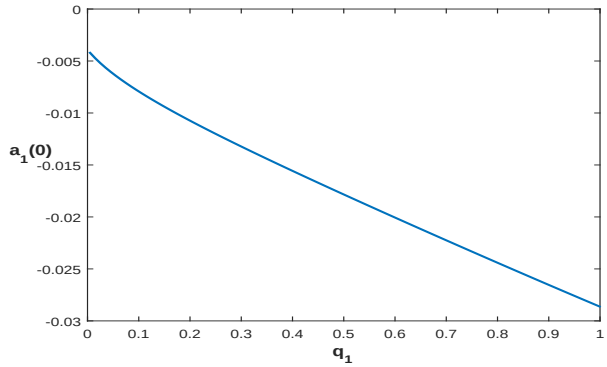

FIGURE 3.1. The plot of the first Lyapunov coefficient $a_1(0)$ as a function of the market fraction of fundamentalists q_1 for the no-switching model (3.3); here $K = 250$, $r = 0.05$, $\bar{D} = 0.02$, $\sigma = 0.2$, $a = a_1 = a_2 = 0.5$, $\mu = 1$, $\alpha = 0.3$, $\gamma = \gamma^{**}$, $\delta = 0.85$, and $b_2 = 0.05$.

3.2. **The Switching Model.** Next we examine the full model (3.1). Though we obtain a very similar result in Theorem 3.2 on the global bifurcation to Theorem 3.1, the dynamics of (3.1) is much richer. In particular, we obtain the coexistence of the locally stable steady state and bifurcated invariant cycles.

Theorem 3.2. *Denote* $\rho = \frac{a_2}{a_1}$, $Q = 2a_2\sigma_1^2(1+r^2)$, $\bar{m} = \tanh\frac{\beta(C_2-C_1)}{2}$, $m_q = n_0 m_0 + (1-n_0)\bar{m}$,

$$M = \frac{\mu}{Q}[\rho(1+m_q)(\alpha - R) + (1-m_q)(1-R)](< 0),$$

and

$$\gamma^{**} = (R-1) + \frac{Q(1-\delta)}{\delta\mu(1-m_q)} + \frac{\rho(1+m_q)(R-\alpha)}{(1-m_q)}, \tag{3.5}$$

(i) *The deterministic system* (3.1) *has a unique fundamental steady state* $(p, u, v, m) = (\bar{p}, \bar{p}, 0, \bar{m})$.

(ii) *Assume* $-2 < M < 0$. *The fundamental steady state* $(\bar{p}, \bar{p}, 0, \bar{m})$ *is locally asymptotically stable for* $\gamma \in (0, \gamma^{**})$, *and it undergoes a Neimark-Sacker bifurcation at* $\gamma = \gamma^{**}$, *that is, there is an invariant curve near the fundamental steady state.*

(iii) *Moreover, the bifurcated closed invariant curve is forward and stable when* $a_2(0) < 0$ *and backward and unstable when* $a_2(0) > 0$, *here the first Lyapunov coefficient* $a_2(0)$ *is given by* (B.11) *in Appendix B.*

Proof. See Appendix B. □

Note that the market fractions of the fundamentalists and trend followers at the fundamental steady state are given by $q_1 = (1 + m_q)/2$ and $q_2 = (1 - m_q)/2$, respectively. The local stability result in Theorem 3.2 shares the same intuition as in Theorem 3.1. In addition, if the cost for the fundamental strategy C_1 is higher than the cost for the trend followers C_2, then an increase in the switching intensity β leads to a decrease in γ^{**}, meaning that the fundamental price becomes less stable when traders switch their strategies more often. This is essentially the rational routes to randomness of Brock and Hommes (1997, 1998). On the dynamics, Fig. 3.2 illustrates two different types of bifurcations.

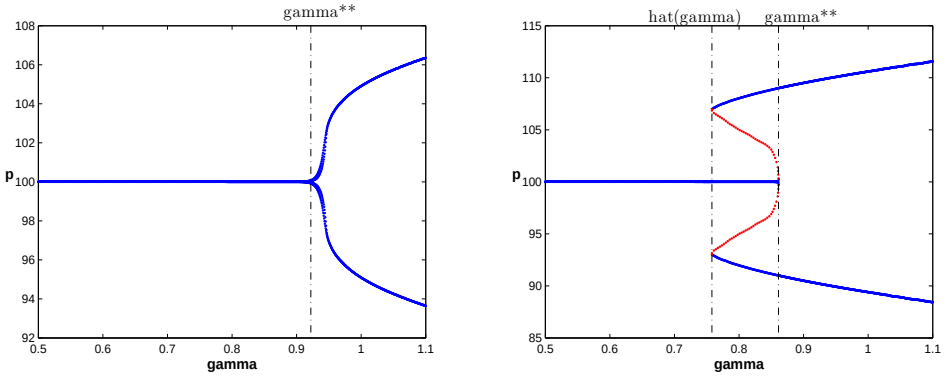

(a) $n_0 = 0.8$ (b) $n_0 = 0.5$

FIGURE 3.2. The bifurcation diagrams of the market price with respect to γ. Here $K = 250$, $r = 0.05$, $\bar{D} = 0.02$, $\sigma = 0.2$, $C = C_1 - C_2 = 0.5$, $a = a_1 = a_2 = 0.5$, $\mu = 1$, $\alpha = 0.3$, $\delta = 0.85$, $\beta = 0.5$, $b_2 = 0.05$, $\gamma = 0.8$, and $m_0 = 0$.

Similar to the previous result, it is the sign of the first Lyapunov coefficient $a_2(0)$ that determines the bifurcation direction, either forward or backward, and the stability of the bifurcated invariant cycles, leading to different bifurcation dynamics. When $a_2(0) < 0$, the bifurcation is forward and stable, meaning that the bifurcated invariant cycle occurring for $\gamma > \gamma^{**}$ is locally stable. In this case, as γ increases and passes γ^{**}, the fundamental steady state becomes unstable and the trajectory converges to an invariant cycle bifurcating from the fundamental steady state. As

γ increases further, the trajectory converges to invariant cycles with different sizes. This is illustrated in Fig. 3.2 (a) with $\gamma^{**} \approx 0.93$ where the two bifurcating curves for $\gamma > \gamma^*$ indicate the minimum and maximum value boundaries of the bifurcating invariant cycles as γ increases.

However, when $a_2(0) > 0$, the bifurcation is backward and unstable, meaning that the bifurcated invariant cycle occurring at $\gamma = \gamma^{**}$ is unstable. This is illustrated in Fig. 3.2 (b) (with $\gamma^{**} \approx 0.88$). There would be a continuation of the unstable bifurcated cycles as γ decreases initially until it reaches a critical value $\hat{\gamma}$, which is indicated by the two red curves of the bifurcating cycles for $\hat{\gamma} < \gamma < \gamma^{**}$. Then as γ increases from the critical value $\hat{\gamma}$, the bifurcation becomes forward and stable. This is illustrated by the two blue curves, which are the boundaries of the bifurcating cycles, for $\gamma > \hat{\gamma}$. Therefore, the stable steady state coexists with the 'forward extended' cycle for $\hat{\gamma} < \gamma < \gamma^{**}$, in between there is a backward extended unstable cycle.[8] For $\hat{\gamma} < \gamma < \gamma^{**}$, even when the fundamental steady state is locally stable, prices need not converge to the fundamental value, may settle down to a stable limit cycle. We call $\hat{\gamma} < \gamma < \gamma^{**}$ the 'volatility clustering region'.

Based on the above analysis, a necessary condition on the coexistence is the positive first Lyapunov coefficient $a_2(0) > 0$. Therefore it is very helpful to understand the condition and economic intuition for various parameters satisfying $a_2(0) > 0$. In the following discussion, we numerically examine this necessary condition and the coexistence.

[8]The global extension of bifurcated cycle can be frequently observed in continuous-time dynamical systems, see for example, He et al. (2009), He and Li (2012, 2015*a*), Di Guilmi, He and Li (2014) and Li (2014). Mathematically, it can be demonstrated that the space $\Sigma = \text{Cl}\{(x, \gamma, l) : (x, \gamma, l) \in X \times R_+ \times R_+\}$ is unbounded (X is the space of the solutions of the system, γ is the examined parameter and l is the period of the cycle), however the solutions of the dynamical system are uniformly bounded and the period is also bounded. Therefore, the space Σ has to be unbounded with respect to the examined parameter γ. In other words, the bifurcated cycle can be globally extended with respect to γ. We refer readers to He et al. (2009) for the details. However, such analysis on the global extension for the discrete-time dynamical system becomes very challenging. This is mainly due to the fact that the bifurcated closed invariant cycle in discrete-time dynamical system has no exact 'period'. However, we demonstrate numerically that the bifurcated closed invariant cycle of our system can also be globally extended.

3.3. **The First Lyapunov Coefficient.** The first Lyapunov coefficient $a_2(0)$ is defined by (B.11) in Appendix B. We have illustrated the main results by using the extrapolation parameter γ of the trend followers. To provide further insights into the mechanism on the coexistence, we examine the dependence of $a_2(0)$ on the market fractions n_o and m_o, the switching intensity β, the decaying rate of the price trend δ, the activity of the fundamentalists α, the risk aversion $a(= a_1 = a_2)$, and the price adjustment of the market maker μ. Unless specified otherwise, all the results are based on the set of parameter values with $K = 250$, $r = 0.05$, $\bar{D} = 0.02$, $\sigma = 0.2$, $C = C_1 - C_2 = 0.5$, $a = a_1 = a_2 = 0.5$, $\mu = 1$, $\alpha = 0.3$, $\gamma = \gamma^{**}$, $\delta = 0.85$, $\beta = 0.5$, $b_2 = 0.05$ and $m_0 = 0$.

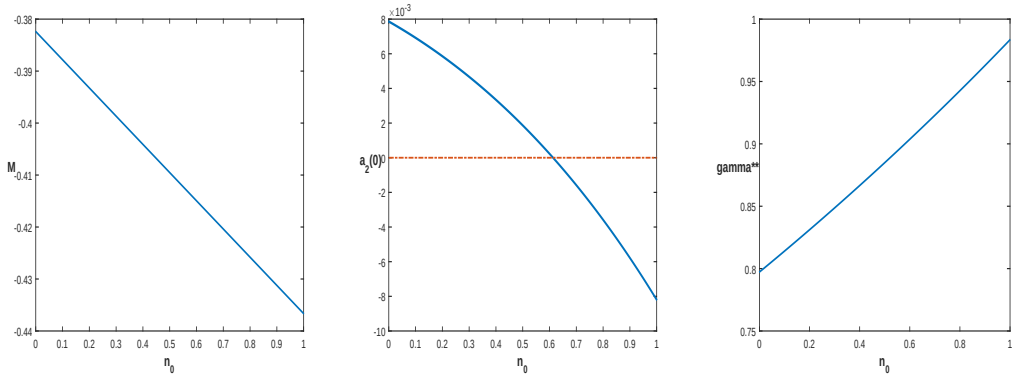

(a) M as a function of n_0 (b) $a_2(0)$ as a function of n_0 (c) γ^{**} as a function of n_0

FIGURE 3.3. The plots of (a) M, (b) the first Lyapunov coefficient for the switching model (3.1) and (c) γ^{**} as a function of n_0. Here $K = 250$, $r = 0.05$, $\bar{D} = 0.02$, $\sigma = 0.2$, $C = C_1 - C_2 = 0.5$, $a = a_1 = a_2 = 0.5$, $\mu = 1$, $\alpha = 0.3$, $\gamma = \gamma^{**}$, $\delta = 0.85$, $\beta = 0.5$, $b_2 = 0.05$ and $m_0 = 0$.

We first consider the effect of n_0, the proportion of investors who do not change their strategies. Fig. 3.3 (a) shows that the condition $-2 < M < 0$ of Theorem 3.2 is always satisfied when n_0 varies from zero to one. Fig. 3.3 (b) illustrates that the volatility clustering interval ($a_2(0) > 0$) for $n_0 < 0.62$. This explains the results of Figs. 3 (c) and (d) in Dieci et al. (2006) who numerically show the coexistence of a stable cycle and a stable steady state when $n_0 = 0.5$ (with the same other parameters). Fig. 3.3 (b) also complements the numerical findings in Dieci et al.

(2006) by providing a wider range of coexistence with respect to n_0. When $n_0 = 0.62$, the first Lyapunov coefficient equals zero as illustrated in Fig. 3.3 (b), and the system (3.1) undergoes a Chenciner (generalized Neimark-Sacker) bifurcation. Fig. 3.3 (c) plots the first Neimark-Sacker bifurcation value γ^{**}. Notice that Theorem 3.2 depicts that the steady state is stable for $0 < \gamma < \gamma^{**}$ and undergoes a Neimark-Sacker bifurcation at $\gamma = \gamma^{**}$. Fig. 3.3 (c) shows that γ^{**} is an increase function of n_0 in this case. This implies that, as more investors switch their trading strategies (that is when n_o decreases), even with the trend followers become less active in the market, the price dynamics is more likely displaying the coexistence. In particular, when there is no agent using fixed strategies and all agents switch their strategies over time ($n_0 = 0$), the system is stable for $0 < \gamma < \gamma^{**}(= 0.79)$ and becomes unstable for $\gamma > \gamma^{**}$. $a_2(0) > 0$ when $\gamma = \gamma^{**}$. However when there is no switching ($n_o = 1$) and all agents use fixed strategies over time ($n_0 = 1$), the stable region increases to $0 < \gamma < \gamma^{**}(= 0.97)$ and $a_2(0) < 0$ when $\gamma = \gamma^{**}$. This implies that, with more agents to switch between two strategies, a weak extrapolation from the trend followers can lead to the coexistence.

On the effect of other parameters, Fig. 3.4 plots of the first Lyapunov coefficient $a_2(0)$ against β, δ α, a and μ. Fig. 3.4 (a) shows that $a_2(0)$ becomes positive when $\beta > 0.4$, implying the coexistence when agents switch between strategies more often. Interestingly, we know from Fig. 3.1 that there is no coexistence when no investor switches; however, Fig. 3.4 (a) and Fig. 3.3 (b) show that when more traders switch their strategies more often, the price dynamics display more coexistence. Fig. 3.4 (b) shows that $a_2(0)$ is positive when $\delta > 0.72$, indicating the coexistence when more weight is given to the past price when calculating the price trend. Fig. 3.4 (c) shows that $a_2(0)$ is positive for medium range of α. This is consistent with the intuition from Gaunersdorfer et al. (2008) that, when the trading activity from the fundamentalists is neither too weak nor too strong, the price can converge to the fundamental value when the trend extrapolation from the trend followers is weak or to an invariant cycle when the extrapolation is strong, leading to the coexistence. Fig. 3.4 (d) and (e) show that $a_2(0)$ becomes positive when $a < 0.6$ or $\mu < 1.2$, indicating the coexistence when agents are less risk averse or the market maker

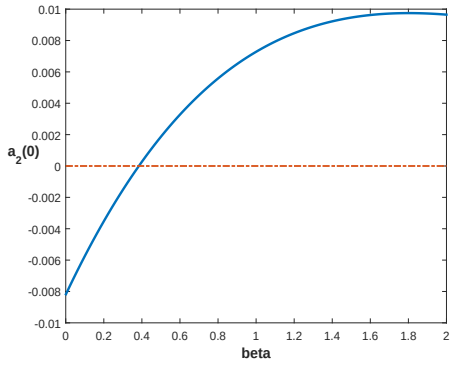

(a) $a_2(0)$ as a function of β

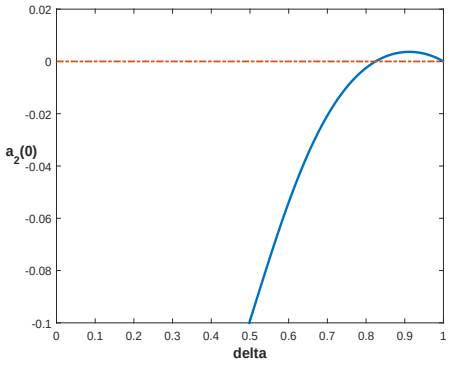

(b) $a_2(0)$ as a function of δ

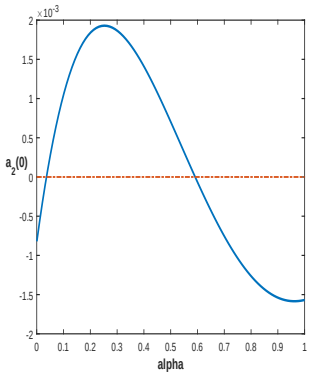

(c) $a_2(0)$ as a function of α

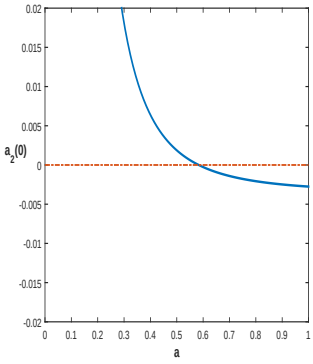

(d) $a_2(0)$ as a function of a

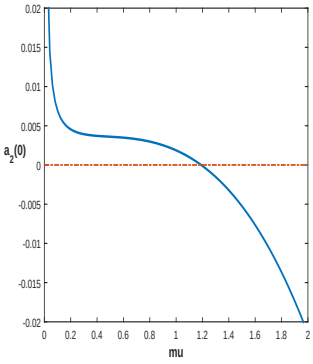

(e) $a_2(0)$ as a function of μ

FIGURE 3.4. The plots of the first Lyapunov coefficient for the switching model (3.1) as a function of (a) β, (b) δ, (c) α, (d) a and (e) μ . Here $K = 250$, $r = 0.05$, $\bar{D} = 0.02$, $\sigma = 0.2$, $C = C_1 - C_2 = 0.5$, $a = a_1 = a_2 = 0.5$ (except for (e)), $\mu = 1$ (except for (d)), $\alpha = 0.3$ (except for (c)), $\gamma = \gamma^{**}$, $\delta = 0.85$ (except for (b)), $\beta = 0.5$ (except for (a)), $b_2 = 0.05$, $n_0 = 0.5$ and $m_0 = 0$.

adjusts the market price weakly. These results based on Fig. 3.4 further verify the simple economic intuition proposed in Gaunersdorfer et al. (2008): *"if traders' sensitivity to differences in fitness is high (i.e. the intensity of choice β is high) then the interaction between weakly extrapolating trend followers (i.e. for large values of decay rate δ) and weakly stabilizing fundamentalists (i.e. with large adjustment speed $1-\alpha$) leads to coexistence of attractors and agents may coordinate on a stable limit cycle around the locally stable fundamental steady state."*

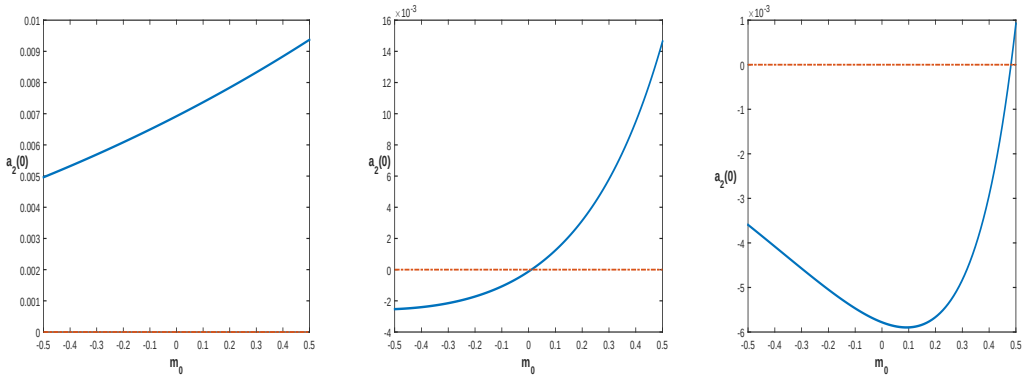

(a) $a_2(0)$ as a function of m_0 where $n_0 = 0.1$ (b) $a_2(0)$ as a function of m_0 where $n_0 = 0.62$ (c) $a_2(0)$ as a function of m_0 where $n_0 = 0.9$

FIGURE 3.5. The plots of the first Lyapunov coefficient for the switching model (3.1) as a function of (a)—(c) m_0, (d)—(f) μ and (g)—(i) $a(= a_1 = a_2)$. Here $K = 250$, $r = 0.05$, $\bar{D} = 0.02$, $\sigma = 0.2$, $C = C_1 - C_2 = 0.5$, $a = a_1 = a_2 = 0.5$ (except for (g-i)), $\mu = 1$ (except for (d-f)), $\alpha = 0.3$, $\gamma = \gamma^{**}$, $\delta = 0.85$, $\beta = 0.5$, $b_2 = 0.05$ and $m_0 = 0$ (except for (a-c)).

We further study the joint impact of m_o and n_o. Figs. 3.5 (a)—(c) show that m_0 can affect the sign of the first Lyapunov coefficient only when n_0 is close to its critical value for the coexistence, $n_0 = 0.62$, as illustrated in Fig. 3.3 (b). When n_0 departs from the critical value 0.62, Figs. 3.5 (a) and (c) show that the sign of $a_2(0)$ becomes less sensitive to the change of m_0.[9] In summary, economically, the above analysis show that when the trading activities of either the fundamental investors or the trend followers dominate the market, market price fluctuates around either the fundamental value with low volatility or a cyclical price movement with high volatility depending on market conditions. When neither the fundamental traders nor the trend followers dominate the market, the fundamental noise and noise traders trigger an irregular shifting between two volatility regimes and therefore leads to volatility clustering. In particular, the effect of volatility clustering becomes more

[9]However, Figs. 3.3 and 3.4 show that n_0, β, δ, α and μ can affect the sign of $a_2(0)$ even when $n_0 = 0.5$, or when n_0 is chosen far away from its critical value, say $n_0 = 0.1$ or 0.9 (not reported here).

significant when traders switch their strategies more often, which is a very different from the mechanism proposed in He and Li (2007).

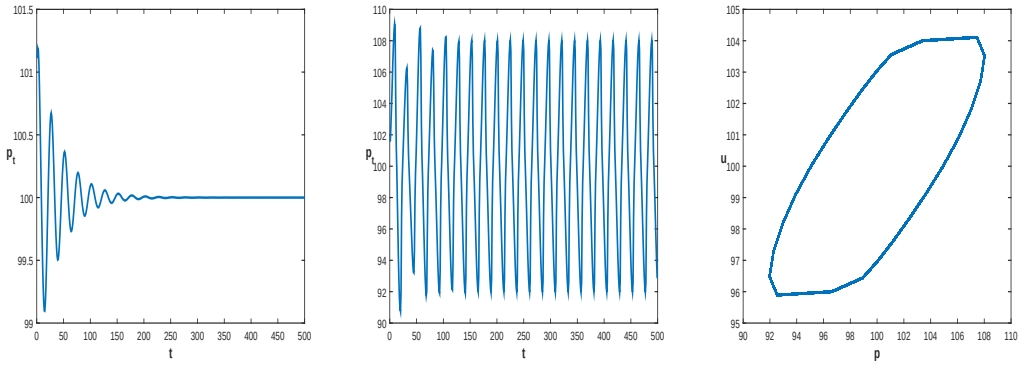

(a) Price time series (b) Price time series (c) phase plot

FIGURE 3.6. (a) The deterministic trajectories of price versus time for (a) $(p_0, u_0, v_0, m_0) = (\bar{p}+1, \bar{p}, 0, \bar{m})$ and (b) $(p_0, u_0, v_0, m_0) = (\bar{p}+1, \bar{p}-1, 0, \bar{m})$ and (c) the phase plot of (p, u). Here $K = 250$, $r = 0.05$, $\bar{D} = 0.02$, $\sigma = 0.2$, $C = C_1 - C_2 = 0.5$, $a = a_1 = a_2 = 0.5$, $\mu = 1$, $\alpha = 0.3$, $\delta = 0.85$, $\beta = 0.5$, $b_2 = 0.05$, $\gamma = 0.8$, $n_0 = 0.5$ and $m_0 = 0$.

3.4. **The Coexistence and Basin of Attraction.** To conclude the analysis of the deterministic dynamics, we numerically verify the coexistence demonstrated by Theorem 3.2. Fig. 3.2(b) illustrates the bifurcation diagram of the market price with respect to γ and demonstrates the global extension of the bifurcated cycle. The blue horizontal line indicates that the steady state is stable for $0 < \gamma < \gamma^{**}(\approx 0.88)$ and undergoes a Neimark-Sacker bifurcation at $\gamma = \gamma^{**}$. Notice $a_2(0) > 0$ when $n_0 = 0.5$ as illustrated in Fig. 3.3 (b). So the bifurcation is backward and the corresponding bifurcated closed invariant cycle is unstable. We plot the unstable cycle using red line, which is extended until $\gamma = \hat{\gamma} \approx 0.76$. Then the bifurcated closed cycle becomes forward and stable. This is illustrated by the two upper and lower blue boundaries of the closed invariant curves with respect to γ, starting from $\hat{\gamma} \approx 0.76$. Therefore, the stable cycle coexists with the stable steady state for $\hat{\gamma} < \gamma < \gamma^{**}$. To demonstrate the coexistence, we plot the deterministic trajectories of price versus time with different initial conditions. First, we choose the initial

values $(p_0, u_0, v_0, m_0) = (\bar{p}+1, \bar{p}, 0, \bar{m}) \approx (101, 100, 0, -0.1244)$, which are their steady state values except for a slightly higher price than the fundamental price. Fig. 3.6 (a) shows that the steady state is locally asymptotically stable in this case. When we decrease the initial point of u_0 to $\bar{p}-1$, slightly smaller than its steady state value, and choose the other parameters the same as those in Fig. 3.6 (a), Figs. 3.6 (b) and (c) illustrate that the price trajectory converges to the closed invariant curve. This coexistence phenomenon is also observed in Dieci et al. (2006).[10]

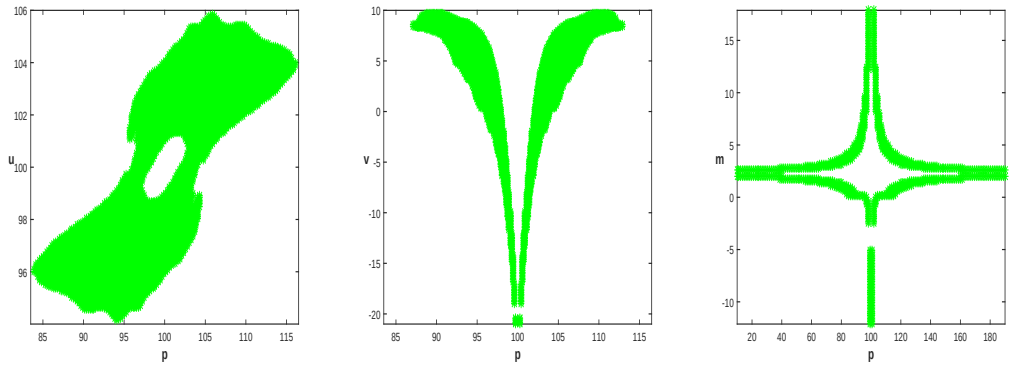

(a) Basin projection on (p, u) space (b) Basin projection on (p, v) space (c) Basin projection on (p, m) space

FIGURE 3.7. The projections of the basin of the two attractors on (a) (p, u) space, (b) (p, v) space and (c) (p, m) space. Here $K = 250$, $r = 0.05$, $\bar{D} = 0.02$, $\sigma = 0.2$, $C = C_1 - C_2 = 0.5$, $a = a_1 = a_2 = 0.5$, $\mu = 1$, $\alpha = 0.3$, $\delta = 0.85$, $\beta = 0.5$, $b_2 = 0.05$, $\gamma = 0.8$, $n_0 = 0.5$ and $m_0 = 0$.

The coexistence of the locally stable steady state and invariant cycle illustrated in Figs. 3.6 (a) and (b) shows that the price dynamics depends on the initial values, or basins of attraction, illustrated in Fig. 3.7. With the set of parameters $K = 250$, $r = 0.05$, $\bar{D} = 0.02$, $\sigma = 0.2$, $C = C_1 - C_2 = 0.5$, $a = a_1 = a_2 = 0.5$, $\mu = 1$, $\alpha = 0.3$, $\delta = 0.85$, $\beta = 0.5$, $b_2 = 0.05$, $\gamma = 0.8$, $n_0 = 0.5$ and $m_0 = 0$, Fig. 3.7 shows that the system only has two attractors, that is, a fundamental steady state and a closed

[10]Under this set of parameters, further numerical simulations suggest that the fundamental steady state (invariant cycle) is globally stable for $\gamma < \hat{\gamma}$ ($\gamma > \gamma^{**}$), and the system (3.1) only has these two attractors for $\hat{\gamma} < \gamma < \gamma^{**}$.

invariant curve extended backward from the bifurcated curve at γ^{**}. The white (light) area indicates the basin of attraction of the fundamental steady state and the green (dark) area is of the closed invariant curve. Both areas are the projection of the basin of attractor $(\bar{p}, \bar{p}, 0, \bar{m})$ on the sub-space of (p, u) in (a), (p, v) in (b), and (p, m) in (c). For example, the green (white) area in Fig. 3.7 (a) illustrates the initial conditions with respect to (p, u) at which the trajectories eventually converge to the closed invariant curve (fundamental steady state) by fixing the initial values of v, m at their steady state values and letting the initial values of p, u vary.[11]

4. Price behavior of the stochastic model

In this section, through numerical simulations, we study the interaction between the coexistence of the deterministic dynamics and the noise processes and explore the potential power of the model to generate various market behavior and the stylized facts, in particular, the volatility clustering and long range dependence in volatility observed in financial markets.

We explore the potential of the stochastic model in generating the stylized facts for daily data observed in financial markets, including volatility clustering and power-law behavior, see He and Li (2007). For the stochastic model with both noise processes, we use the same set of parameters as in Section 3 to guarantee the coexistence of two locally stable attractors. The volatilities of the market price process and fundamental price process are chosen as $\sigma_\delta = 2$ and $\sigma_\epsilon = 0.025$, respectively. Fig. 4.1 represents the results of a typical simulation. Fig. 4.1 (a) shows that the market price (the red solid line) follows the fundamental price (the blue dotted line) in general, but accompanied with large deviations from time to time. With the

[11]Strictly speaking, the green (white) areas in Figs. 3.7 (a)—(c) are not exactly the projection of the basin of the closed invariant curve (fundamental steady state) on different sub-space because we plot them versus the initial values for two variables by fixing those of the other two, rather than plot the basin of attraction by letting all variables' initial values vary versus a sub-space. For convenience, we call it as 'projection' in this paper. Also notice that there can be more than one green (white) area in each plot. However, they are generated from the same basin of the closed invariant curve (fundamental steady state) on a sub-space. Because the system is a 4-dimensional, the projection on a sub-space may be divided into multiple areas.

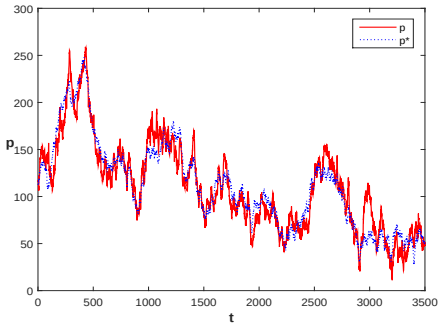

(a) The market price and the fundamental price

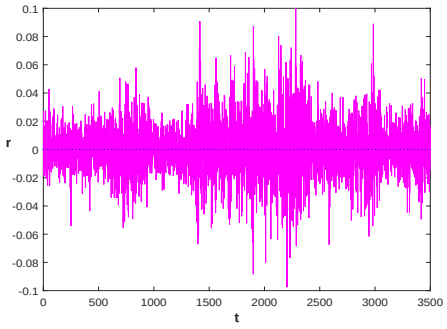

(b) The market returns (r)

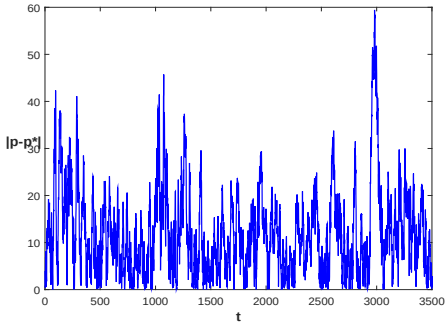

(c) The deviation of prices $|p_t - p_t^*|$

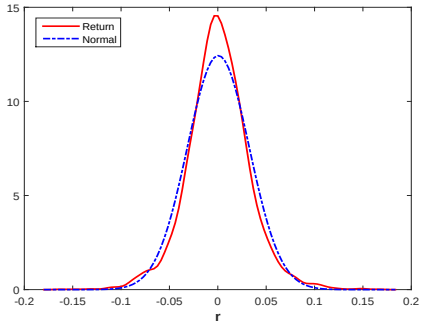

(d) The density of the market returns

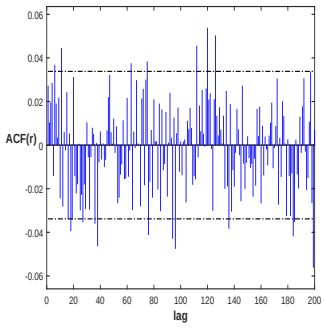

(e) The ACs of the market returns

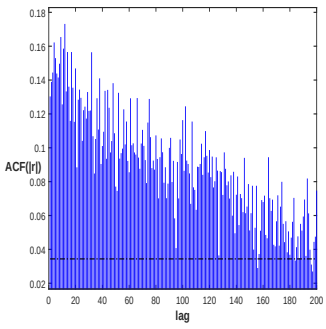

(f) The ACs of the absolute returns

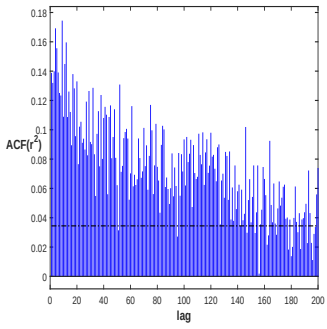

(g) The ACs of the squared returns

FIGURE 4.1. The time series of (a) the market price (red solid line) and the fundamental price (blue dotted line), (b) the market returns; and (c) the deviation of market price from its fundamental $|p_t - p_t^*|$; (d) the return distribution; the ACs of (e) the returns; (f) the absolute returns, and (g) the squared returns. Here $K = 250$, $r = 0.05$, $\bar{D} = 0.02$, $\sigma = 0.2$, $C = C_1 - C_2 = 0.5$, $a = a_1 = a_2 = 0.5$, $\mu = 1$, $\alpha = 0.3$, $\delta = 0.85$, $\beta = 0.5$, $b_2 = 0.05$, $\gamma = 0.8$, $n_0 = 0.5$, $m_0 = 0$, $\sigma_\delta = 2$ and $\sigma_\epsilon = 0.025$.

coexistence of a locally stable steady state and a locally stable limit cycle of the deterministic model shown in Section 3 and the presence of noises, the evolutionary price dynamics then switches irregularly between a phase close to the fundamental steady state with small amplitude price fluctuations and a phase with large price fluctuations along a (noisy) limit cycle. The market returns in Fig. 4.1 (b) show significant volatility clustering. The deviation of market price from fundamental price in Fig. 4.1 (c) is consistent with the pattern of volatility clustering, illustrated by the large volatility in (b) and the big spike in the deviation $|p_t - p_t^*|$ in (c) for t around $t = 3000$. Comparing to the corresponding normal distribution, the return distribution in Fig. 4.1 (d) displays high kurtosis. The returns show almost insignificant autocorrelations (ACs) in Fig. 4.1 (e), but the ACs for the absolute returns and the squared returns in Figs. 4.1 (f) and (g) are significant with strong decaying patterns as time lag increases, implying a long range dependence. These results demonstrate that the stochastic model established in this paper can generate most of the stylized facts observed in financial markets.

The above features of the stochastic model is a joint outcome of the interaction of the nonlinear HAM and the two noisy processes, similar to He and Li (2007). With the same random seeds, we report the simulation results in Figs. 4.2 and 4.3 when there is only one stochastic process involved. In Fig. 4.2, there is no market noise and the fundamental price is the only stochastic process. The time series, return density distribution, and the ACs of the returns, the absolute returns and the squared returns do not replicate these stylized facts demonstrated in Fig. 4.1. Alternatively, in Fig. 4.3 the market noise process is the only stochastic process. It shows that the return is basically described by a white noise process. Both Figs 4.2 and 4.3 indicate that the potential of the model in generating the stylized facts is not due to either one of the two stochastic processes, but to both noisy processes. The underlying mechanism in generating the stylized facts, long range dependence, and the interplay between the nonlinear deterministic dynamics and noises are very similar to the one explored in He and Li (2007). Economically, the fundamental noise can be very different from the market noise coming from the noise traders and consequently they affect the market price differently. Without the market noise,

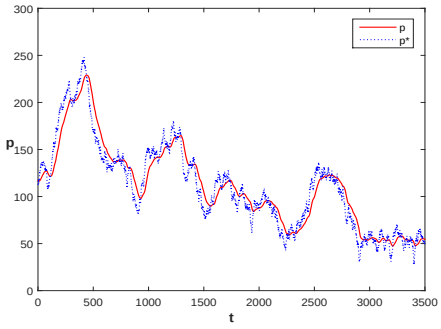

(a) The market price and the fundamental price

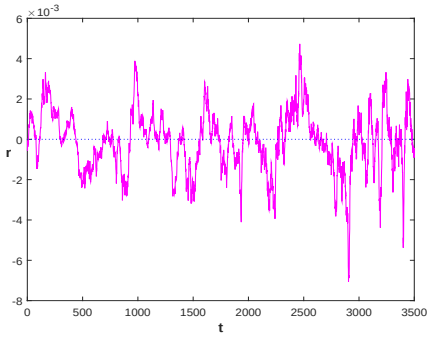

(b) The market returns (r)

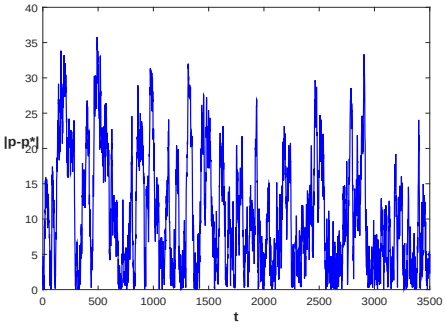

(c) The deviation of prices $|p_t - p_t^*|$

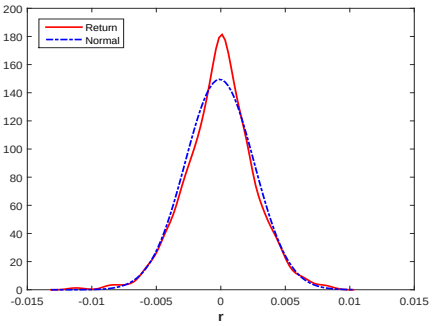

(d) The density of the market returns

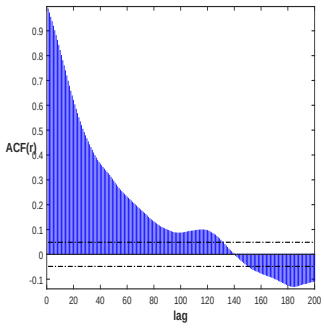

(e) The ACs of the market returns

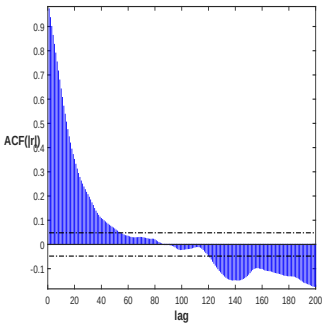

(f) The ACs of the absolute returns

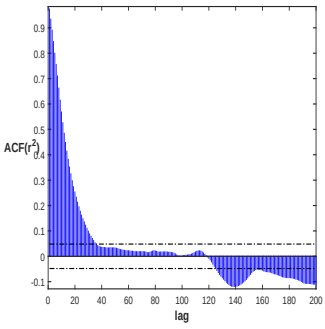

(g) The ACs of the squared returns

FIGURE 4.2. The time series of (a) the market price (red solid line) and the fundamental price (blue dotted line), (b) the market returns; and (c) the deviation of market price from its fundamental $|p_t - p_t^*|$; (d) the return distribution; the ACs of (e) the returns; (f) the absolute returns, and (g) the squared returns. Here $K = 250$, $r = 0.05$, $\bar{D} = 0.02$, $\sigma = 0.2$, $C = C_1 - C_2 = 0.5$, $a = a_1 = a_2 = 0.5$, $\mu = 1$, $\alpha = 0.3$, $\delta = 0.85$, $\beta = 0.5$, $b_2 = 0.05$, $\gamma = 0.8$, $n_0 = 0.5$, $m_0 = 0$, $\sigma_\delta = 0$ and $\sigma_\epsilon = 0.025$.

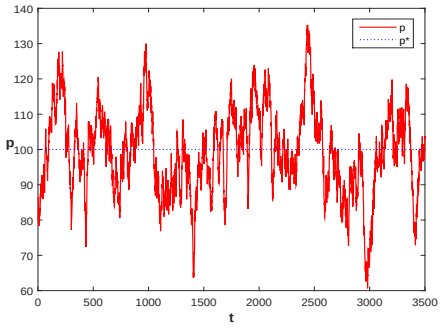

(a) The market price and the fundamental price

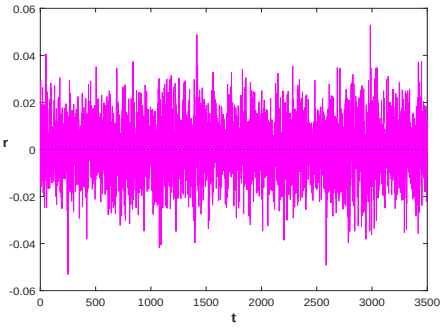

(b) The market returns (r)

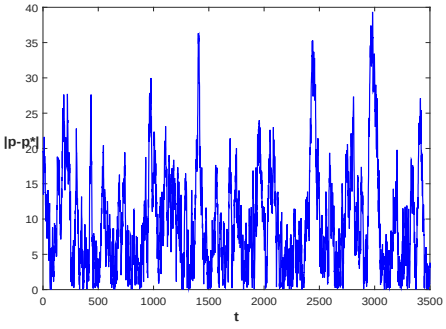

(c) The deviation of prices $|p_t - p_t^*|$

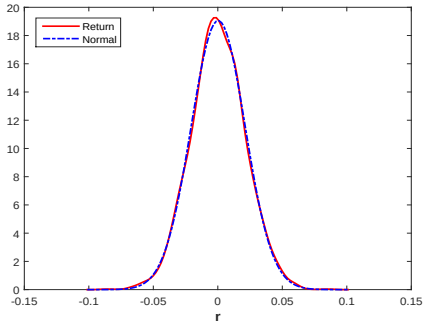

(d) The density of the market returns

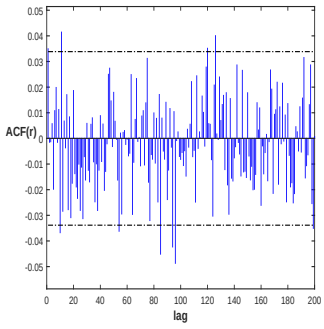

(e) The ACs of the market returns

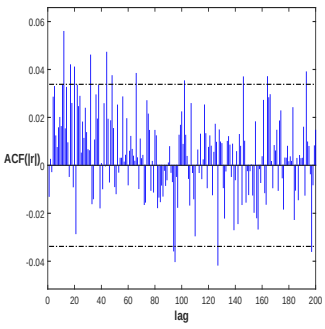

(f) The ACs of the absolute returns

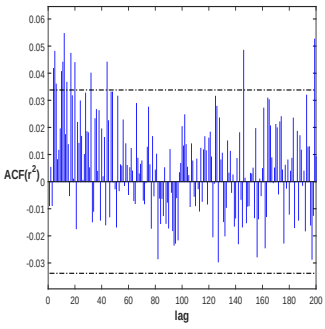

(g) The ACs of the squared returns

FIGURE 4.3. The time series of (a) the market price (red solid line) and the fundamental price (blue dotted line), (b) the market returns; and (c) the deviation of market price from its fundamental $|p_t - p_t^*|$; (d) the return distribution; the ACs of (e) the returns; (f) the absolute returns, and (g) the squared returns. Here $K = 250$, $r = 0.05$, $\bar{D} = 0.02$, $\sigma = 0.2$, $C = C_1 - C_2 = 0.5$, $a = a_1 = a_2 = 0.5$, $\mu = 1$, $\alpha = 0.3$, $\delta = 0.85$, $\beta = 0.5$, $b_2 = 0.05$, $\gamma = 0.8$, $n_0 = 0.5$, $m_0 = 0$, $\sigma_\delta = 2$ and $\sigma_\epsilon = 0$.

the market price are driven by the mean-reverting of the fundamentalists (to the fundamental price) and the trend chasing of the chartists; both contribute to building up market price trend. Due to the randomness of the fundamental price, there are persistent mean-reverting activities from the fundamentalists that provide the chartists opportunities to explore the price trend. Therefore, the significant ACs of the market returns, absolute returns and squared returns in Fig. 4.2 reflect the interaction of the fundamentalists and the trend followers. However, with the market noise and a constant fundamental price, the price trend is less likely formed and explored by the chartists. This limits the impact of the speculative behavior of the chartists, which explains the insignificant ACs of the market returns, absolute returns and squared returns in Fig. 4.3. With both noise processes, the price trend is difficult to explore (due to the market noise) and consequently the returns become less predictable. However, the interaction of the fundamentalists and trend followers becomes intensive due to some large changes in the fundamental price from time to time, implying the significant ACs in return volatility, shown in Fig. 4.1 (e)-(g).

5. Conclusion

This paper contributes to the volatility clustering literature and the development of financial market modelling and asset price dynamics with heterogeneous agents. We consider a simple asset pricing model with two types of boundedly rational traders, fundamentalists and trend followers, and noise traders. By applying the normal form method and the center manifold theory, we obtain analytical conditions on the coexistence of a stable steady state and a stable closed invariant cycle and provide a systematic way to identify volatility clustering interval by examining the stability of a Neimark-Sacker bifurcation through the change of one parameter. When buffered with noises, we then show numerically that the interaction of the coexistence of the deterministic dynamics and noise processes can endogenously generate volatility clustering and long range dependence in volatility observed in financial markets. Economically, with strong trading activities of either the fundamental investors or the trend followers, market price fluctuates around either the

fundamental value with low volatility or a cyclical price movement with high volatility depending on market condition. With the fundamental noise and noise traders, this triggers an irregular shifting between two volatility regimes and therefore leads to volatility clustering. We therefore verify the endogenous mechanism on volatility clustering proposed by Gaunersdorfer et al. (2008) and provide an economic explanation on the volatility clustering. The analysis sheds light on the understanding of volatility clustering. The method developed in this paper can be easily applied to other nonlinear financial and economic models. This helps to provide deep understanding of the globally nonlinear properties of the financial and economic systems.

Appendix A. Stability and Bifurcation Analysis of the Constant Market Fraction Model

Let $w_t = p_{t+1}$, then (3.3) becomes

$$\begin{cases} w_t = w_{t-1} + \mu q_1 \dfrac{(\alpha - R)(w_{t-1} - \bar{p})}{2a_1\sigma_1^2(1+r^2)} + \mu q_2 \dfrac{\gamma(w_{t-1} - u_t) - (R-1)(w_{t-1} - \bar{p})}{2a_2\sigma_1^2(1+r^2+bv_t)}, \\ u_t = \delta u_{t-1} + (1-\delta)\, w_{t-1}, \\ v_t = \delta v_{t-1} + \delta\,(1-\delta)\,(w_{t-1} - u_{t-1})^2\,, \end{cases} \tag{A.1}$$

which is equivalent to the following 3-d map: $T(w,u,v) \to (w',u',v')$

$$\begin{cases} w' = w + \mu q_1 \dfrac{(\alpha - R)(w - \bar{p})}{2a_1\sigma_1^2(1+r^2)} + \mu q_2 \dfrac{\gamma\delta(w-u) - (R-1)(w - \bar{p})}{2a_2\sigma_1^2[1+r^2+b\delta v + b\delta(1-\delta)(w-u)^2]}, \\ u' = \delta u + (1-\delta)\, w, \\ v' = \delta v + \delta\,(1-\delta)\,(w-u)^2\,, \end{cases} \tag{A.2}$$

It is straightforward to see that $(\bar{p}, \bar{p}, 0)$ is an equilibrium of (A.2). Denote $\rho = \frac{a_2}{a_1}$, $Q = 2a_2\sigma_1^2(1+r^2)$. The Jacobian matrix of the function in right-hand side of (A.2) at this equilibrium is given by

$$J = \begin{pmatrix} J_{11}(\gamma) & J_{12}(\gamma) & 0 \\ 1-\delta & \delta & 0 \\ 0 & 0 & \delta \end{pmatrix}, \tag{A.3}$$

where

$$J_{11}(\gamma) = 1 + \frac{\mu}{Q}[q_1\rho(\alpha - R) + q_2(\gamma\delta + 1 - R)],\ J_{12}(\gamma) = -\frac{\mu q_2\gamma\delta}{Q}.$$

The characteristic equation of J is

$$[\lambda^2 + A(\gamma)\lambda + B(\gamma)](\lambda - \delta) = 0 \tag{A.4}$$

with

$$A(\gamma) = -\left[1 + \delta + \frac{\mu}{Q}[q_1\rho(\alpha - R) + q_2(\gamma\delta + 1 - R)]\right],$$
$$B(\gamma) = \delta\left[1 + \frac{\mu}{Q}[q_1\rho(\alpha - R) + q_2(\gamma + 1 - R)]\right].$$

Denote

$$\begin{cases} \gamma^* = (R-1) + \dfrac{Q(1-\delta)}{\delta\mu q_2} - \dfrac{\rho q_1(\alpha - R)}{q_2}, \\ K = \dfrac{\mu}{Q}[q_1\rho(\alpha - R) + q_2(1-R)] < 0. \end{cases} \tag{A.5}$$

Then, the distribution of the roots of (A.4) is described by the following theorem if we use γ as variable parameter.

Lemma A.1. *Suppose $-2 < K < 0$. Then, all the roots of* (A.4) *lie inside of the unit circle for $\gamma \in [0, \gamma^*)$, and there is a pair of conjugate roots, $\cos\theta_0 \pm i\sin\theta_0$ for some $\theta_0 \in (0, \pi/2)$, of* (A.4) *when $\gamma = \gamma^*$.*

Proof. When $\gamma = 0$, the roots of (A.4) are

$$\lambda_1 = 1 + K, \ \lambda_2 = \lambda_3 = \delta.$$

Therefore, $-1 < \lambda_1, \lambda_2, \lambda_3 < 1$. Suppose $\lambda = \cos\theta_0 \pm i\sin\theta_0$, $\theta_0 \in (0, \pi)$, is a root of (A.4). Then

$$\begin{aligned} 2\sin\theta_0\cos\theta_0 + A\sin\theta_0 = 0, \\ \cos^2\theta_0 - \sin^2\theta_0 + A\cos\theta_0 + B = 0, \end{aligned} \tag{A.6}$$

which holds for $B = 1$, or equivalently, $\gamma = \gamma^*$. Substituting γ^* into $A(\gamma)$, we know $A(\gamma^*) = -(2 + (1-\delta)K)$. This implies that $\cos\theta_0 = -\frac{A(\gamma^*)}{2} \in (\delta, 1)$. Therefore, $\theta_0 \in (0, \pi/2)$. □

Lemma A.2. *Suppose $\rho(\gamma)(\cos\theta(\gamma) \pm i\sin\theta(\gamma))$ be the roots of* (A.4) *satisfying $\rho(\gamma^*) = 1$ and $\theta(\gamma^*) = \theta_0$. Then, $\rho'(\gamma^*) > 0$.*

Proof. Differentiating

$$\begin{aligned} \lambda(\gamma) = \rho(\gamma)(\cos\theta(\gamma) + i\sin\theta(\gamma)), \\ 0 = \lambda(\gamma)^2 + A(\gamma)\lambda(\gamma) + B(\gamma), \end{aligned}$$

with respect to γ, respectively, we have

$$\lambda'(\gamma) = \rho'(\gamma)\cos\theta(\gamma) - \rho(\gamma)\theta'(\gamma)\sin\theta(\gamma) + i\rho'(\gamma)\sin\theta(\gamma) + i\rho(\gamma)\theta'(\gamma)\cos\theta(\gamma), \tag{A.7}$$

and

$$\begin{aligned}\lambda'(\gamma) &= -\frac{B'(\gamma)+A'(\gamma)\lambda(\gamma)}{2\lambda(\gamma)+A(\gamma)}\\ &= -\frac{B'(\gamma)+A(\gamma)\rho(\gamma)(\cos\theta(\gamma)+i\sin\theta(\gamma))}{A(\gamma)+2\rho(\gamma)(\cos\theta(\gamma)+i\sin\theta(\gamma))} \qquad \text{(A.8)}\\ &= M(\gamma)+iN(\gamma),\end{aligned}$$

where

$$M(\gamma) = \frac{-(B'(\gamma)+A'(\gamma)\rho(\gamma)\cos\theta(\gamma))(A(\gamma)+2\rho(\gamma)\cos\theta(\gamma)) - 2A'(\gamma)\rho^2(\gamma)\sin^2\theta(\gamma)}{(A(\gamma)+2\rho(\gamma)\cos\theta(\gamma))^2+(2\rho(\gamma)\sin\theta(\gamma))^2},$$

$$N(\gamma) = \frac{2\rho(\gamma)\sin\theta(\gamma)(B'(\gamma)+A'(\gamma)\rho(\gamma)\cos\theta(\gamma)) - (A(\gamma)+2\rho(\gamma)\cos\theta(\gamma))A'(\gamma)\rho(\gamma)\sin\theta(\gamma)}{(A(\gamma)+2\rho(\gamma)\cos\theta(\gamma))^2+(2\rho(\gamma)\sin\theta(\gamma))^2}.$$

From (A.7) and (A.8), we get

$$\begin{aligned}M(\gamma) &= \rho'(\gamma)\cos\theta(\gamma) - \rho(\gamma)\theta'(\gamma)\sin\theta(\gamma),\\ N(\gamma) &= \rho'(\gamma)\sin\theta(\gamma) + \rho(\gamma)\theta'(\gamma)\cos\theta(\gamma)\end{aligned}$$

which implies

$$\rho'(\gamma) = M(\gamma)\cos\theta(\gamma) + N(\gamma)\sin\theta(\gamma).$$

Using the fact that $\rho(\gamma^*)=1$, $B'(\gamma^*)=\frac{\delta\mu q_2}{a_1\sigma_1^2(1+r^2)}>0$ and $A(\gamma^*)+2\rho(\gamma^*)\cos\theta(\gamma^*)=0$, we know

$$\begin{aligned}\mathrm{Sign}\{\rho'(\gamma^*)\} &= \mathrm{Sign}\{-2A'(\gamma^*)\rho^2(\gamma^*)\sin^2\theta(\gamma^*)\cos\theta(\gamma^*)\\ &\quad + 2\rho(\gamma^*)\sin^2\theta(\gamma^*)(B'(\gamma^*)+A'(\gamma^*)\rho(\gamma^*)\cos\theta(\gamma^*))\}\\ &= \mathrm{Sign}\{2B'(\gamma^*)\sin^2\theta(\gamma^*)\} > 0.\end{aligned}$$

□

From Lemmas A.1 and A.2, we obtain the following results on occurence of Neimark-Sacker bifurcation.

Theorem A.3. *Assume $-2 < K < 0$. The equilibrium $(\bar{p},\bar{p},0)$ of Eq. (A.2) is asymptotically stable if $\gamma \in (0,\gamma^*)$, and Eq. (A.2) undergoes a Neimark-Sacker bifurcation at $\gamma=\gamma^*$, that is, there is an isolated closed invariant curve near the origin. Moreover, the bifurcation is forward(backward) and the bifurcated closed invariant curve is stable (unstable) if $a_1(0)<0 (a_1(0)>0)$.*

The first Lyapunov coefficient $a_1(0)$ is computed as below, following the algorithm in p.178 of Kuznetsov (2004). Let q and $\tilde{p}$ be the eigenvectors of J and J' with respect to $e^{i\theta_0}$ and $e^{-i\theta_0}$ respectively. Then

$$q = \begin{pmatrix} \frac{e^{i\theta_0}-\delta}{1-\delta} \\ 1 \\ 0 \end{pmatrix}, \ \tilde{p} = \begin{pmatrix} \frac{e^{-i\theta_0}-\delta}{J_{12}(\gamma^*)} \\ 1 \\ 0 \end{pmatrix}.$$

Set $p = c\tilde{p}$ with

$$c = \frac{(1-\delta)J_{12}(\gamma^*)}{(e^{-i\theta_0}-\delta)^2 + (1-\delta)J_{12}(\gamma^*)}.$$

Then, $< p, q >= \sum_{i=1}^{3} \bar{p}_i q_i = 1$. Recall that the nonlinear term of (A.2) takes the form

$$f(w,u,v) = \begin{pmatrix} \mu q_2 \frac{\gamma\delta(w-u)-(R-1)(w-\bar{p})}{2a_2\sigma_1^2[1+r^2+b\delta v+b\delta(1-\delta)(w-u)^2]} \\ 0 \\ \delta(1-\delta)(w-u)^2 \end{pmatrix} = \begin{pmatrix} f^1 \\ f^2 \\ f^3 \end{pmatrix}. \tag{A.9}$$

The second and third order partial derivatives of f at $(\bar{p}, \bar{p}, 0)$, when $\gamma = \gamma^*$, are

$$f^1_{ww} = f^1_{uu} = f^1_{vv} = f^1_{wu} = f^1_{uw} = 0,$$

$$f^1_{wv} = f^1_{vw} = c_1(\gamma^*\delta + 1 - R), \ f^1_{uv} = f^1_{vu} = c_2\gamma^*\delta,$$

$$f^3_{ww} = f^3_{uu} = 2\delta(1-\delta), f^3_{wu} = -2\delta(1-\delta),$$

and

$$f^1_{www} = 6c_1(\gamma^*\delta + 1 - R)(1-\delta), \ f^1_{wuu} = 2c_1(3\gamma^*\delta + 1 - R)(1-\delta),$$

$$f^1_{uuu} = 6c_2(1-\delta)\gamma^*\delta, \ f^1_{wwu} = 2c_2(3\gamma^*\delta + 2 - 2R)(1-\delta)$$

$$f^1_{vvv} = f^1_{wwv} = f^1_{uuv} = f^1_{wuv} = 0,$$

$$f^1_{wvv} = -\frac{2b\delta c_1(\gamma^*\delta + 1 - R)}{1+r^2}, \ f^1_{uvv} = -\frac{2b\delta c_2\gamma^*\delta}{1+r^2},$$

with

$$c_1 = -\frac{\mu q_2 b\delta}{Q(1+r^2)}, \ c_2 = \frac{\mu q_2 b\delta}{Q(1+r^2)}.$$

For $i_1, i_2, \cdots, i_s$, $i_j \in \mathbb{N}$, $j = 1, 2, \cdots, s$, denote by $(i_1, i_2, \cdots, i_s)$ the set of all permutations of $i_1 i_2 \cdots i_s$. For instance, $(1,2,3) = \{123, 132, 213, 231, 312, 321\}$. Then we can rewrite (A.9) as

$$f = \frac{1}{2}B(x,x) + \frac{1}{6}C(x,x,x) + O(\|x\|\|^4),$$

where $B(x,y)$ and $C(x,y,z)$ are symmetric multilinear vector functions of $x,y,z \in \mathbb{R}^3$, and given by

$$B(x,y) = \begin{pmatrix} f^1_{wv}\Sigma_{ij\in(1,3)}x_iy_j + f^1_{uv}\Sigma_{ij\in(2,3)}x_iy_j \\ 0 \\ f^3_{ww}x_1y_1 + f^3_{uu}x_2y_2 + f^3_{wu}\Sigma_{ij\in(1,2)}x_iy_j \end{pmatrix}$$

and

$$C(x,y,z) = \begin{pmatrix} f^1_{www}x_1y_1z_1 + f^1_{uuu}x_2y_2z_2 + f^1_{wwu}\Sigma_{ijk\in(1,1,2)}x_iy_jz_k \\ +f^1_{wuu}\Sigma_{ijk\in(1,2,2)}x_iy_jz_k + f^1_{uvv}\Sigma_{ijk\in(2,3,3)}x_iy_jz_k + f^1_{wvv}\Sigma_{ijk\in(1,3,3)}x_iy_jz_k \\ 0 \\ 0 \end{pmatrix}$$

Therefore, the first Lyapunov coefficient $a_1(0)$ is given by

$$\begin{aligned} a_1(0) &= \frac{1}{2}\mathrm{Re}\left\{e^{-i\theta_0}[< p, C(q,q,\bar{q}) > +2 < p, B(q,(E-J)^{-1}B(q,\bar{q})) > \right. \\ &\qquad \left. + < p, B(\bar{q},(e^{2i\theta_0}E - J)^{-1}B(q,q)) >]\right\} \\ &= \frac{1}{2}\mathrm{Re}\left\{\frac{\bar{c}(1-\delta e^{-i\theta_0})}{J_{12}(\gamma^*)}\left[K_3 + \left(\frac{(e^{-i\theta_0}-\delta)}{(1-\delta)}f^1_{wv} + f^1_{uv}\right)(2K_1 + K_2)\right]\right\} \end{aligned} \tag{A.10}$$

where

$$\begin{aligned} K_1 &= 2\delta\left[\frac{(e^{i\theta_0}-\delta)(e^{-i\theta_0}-\delta)}{(1-\delta)^2} - \frac{(e^{i\theta_0}-e^{-i\theta_0})}{1-\delta} + 1\right], \\ K_2 &= \frac{2\delta(1-\delta)}{e^{2i\theta_0}-\delta}\left[\left(\frac{e^{i\theta_0}-\delta}{1-\delta}\right)^2 - \frac{2(e^{i\theta_0}-\delta)}{1-\delta} + 1\right], \\ K_3 &= \frac{(e^{i\theta_0}-\delta)^2(e^{-i\theta_0}-\delta)}{(1-\delta)^3}f^1_{www} + f^1_{uuu} + \left[\left(\frac{e^{i\theta_0}-\delta}{1-\delta}\right)^2 + \frac{2(e^{i\theta_0}-\delta)(e^{-i\theta_0}-\delta)}{(1-\delta)^2}\right]f^1_{wwu} \\ &\quad + \left(\frac{e^{-i\theta_0}-\delta}{1-\delta} + \frac{2(e^{i\theta_0}-\delta)}{1-\delta}\right)f^1_{wuu} \end{aligned}$$

Appendix B. Stability and Neimark-Sacker Bifurcation of the Evolution Model

The whole system is

$$\begin{cases} p' = p + \dfrac{\mu}{2}\{[n_0(1+m_0) \\ \qquad\qquad + (1-n_0)(1+m)]z_1 + [n_0(1-m_0) + (1-n_0)(1-m)]z_2\}, \\ u' = \delta u + (1-\delta)p', \\ v' = \delta v + \delta(1-\delta)(p'-u)^2, \\ m' = \tanh\left\{\dfrac{\beta}{2}[(z_1-z_2)(p'+\bar{D}-Rp) - C_1 + C_2]\right\}, \end{cases} \tag{B.1}$$

where

$$\begin{aligned} z_1 &= z_1(p) = \frac{(\alpha - R)(p-\bar{p})}{a_1\sigma_1^2(1+r^2)}, \\ z_2 &= z_2(p,u,v) = \frac{\gamma(p-u) - (R-1)(p-\bar{p})}{a_2\sigma_1^2(1+r^2+bv)}, \end{aligned} \tag{B.2}$$

The positive equilibrium of (B.1) is given by $E = (\bar{p}, \bar{p}, 0, \bar{m})$ with $\bar{p} = \frac{\bar{D}}{R-1}$ and $\bar{m} = \tanh\frac{\beta(C_2-C_1)}{2}$. Denote $\rho = \frac{a_2}{a_1}$, $Q = 2a_2\sigma_1^2(1+r^2)$, and $m_q = n_0m_0 + (1-n_0)\bar{m}$. The matrix associated with the linearized system of (B.1) at E is

$$J = \begin{pmatrix} G_1 & 0 \\ 0 & G_2 \end{pmatrix}$$

where

$$G_1 = \begin{pmatrix} \frac{\partial p'}{\partial p} & \frac{\partial p'}{\partial u} \\ (1-\delta)\frac{\partial p'}{\partial p} & \delta + (1-\delta)\frac{\partial p'}{\partial u} \end{pmatrix} := \begin{pmatrix} G_{11}(\gamma) & G_{12}(\gamma) \\ G_{21}(\gamma) & G_{22}(\gamma) \end{pmatrix} \tag{B.3}$$

with

$$\begin{aligned} \frac{\partial p'}{\partial p} &= 1 + \frac{\mu(1-m_q)}{Q}[\rho(\alpha - R) - (\gamma + 1 - R)], \\ \frac{\partial p'}{\partial u} &= -\frac{\gamma\mu(1-m_q)}{Q} \end{aligned}$$

and

$$G_2 = \begin{pmatrix} \delta & 0 \\ 0 & 0 \end{pmatrix} \tag{B.4}$$

It is obvious that the eigenvalues of G_2 are δ and 0. It remains to investigate the eigenvalues of G_1. Define

$$\begin{aligned} \gamma^{**} &= (R-1) + \frac{Q(1-\delta)}{\delta\mu(1-m_q)} - \frac{\rho(1+m_q)(\alpha-R)}{(1-m_q)}, \\ M &= \frac{\mu}{Q}[\rho(1+m_q)(\alpha-R) + (1-m_q)(1-R)] < 0. \end{aligned} \tag{B.5}$$

Using a similar argument as in Section A, we arrive at the following results

Lemma B.1. *Suppose $-2 < M < 0$. Then, all the eigenvalues of G_1 lie in the unit circle for $\gamma \in [0, \gamma^{**})$, and G_1 has a pair of conjugate roots, $\cos\theta_0 \pm i\sin\theta_0$ for some $\theta_0 \in (0, \pi/2)$, when $\gamma = \gamma^{**}(> 0)$.*

Lemma B.2. *Suppose $\rho(\gamma)(\cos\theta(\gamma) \pm i\sin\theta(\gamma))$ be the eigenvalues of G_1 satisfying $\rho(\gamma^{**}) = 1$ and $\theta(\gamma^{**}) = \theta_0$. Then, Sign$\{\rho'(\gamma^{**})\}$ = Sign$(1 - m_q)$.*

It can be verified that $m_q < 1$ and hence $\text{Sign}\{\rho'(\gamma^{**})\} > 0$.

Theorem B.3. *Assume $-2 < M < 0$. The equilibrium $(\bar{p}, \bar{p}, 0, \bar{m})$ of Eq.*(B.1) *is asymptotically stable if $\gamma \in (0, \gamma^{**})$, and Eq.* (B.1) *undergoes a Neimark-Sacker bifurcation at $\gamma = \gamma^{**}$, that is, there is an isolated closed invariant curve near the origin. Moreover, the bifurcation is forward(backward) if Sign$\{\rho'(\gamma^{**})\}/a_2(0) < 0$(Sign$\{\rho'(\gamma^{**})\}/a_2(0) > 0$), and the bifurcated closed invariant curve is stable(unstable) if $a_2(0) < 0$($a_2(0) > 0$).*

To compute the first Lyapunov coefficient $a_2(0)$. The following quantities are needed. The eigenvectors of J and J' associated with $e^{i\theta_0}$ and $e^{-i\theta_0}$ are

$$q = \begin{pmatrix} \frac{G_{12}}{e^{i\theta_0} - G_{11}} \\ 1 \\ 0 \\ 0 \end{pmatrix}, \; p = c \begin{pmatrix} \frac{(1-\delta)G_{11}}{e^{-i\theta_0} - G_{11}} \\ 1 \\ 0 \\ 0 \end{pmatrix}, \tag{B.6}$$

where

$$G_{11}(\gamma^{**}) = \frac{1}{\delta}, \; G_{12}(\gamma^{**}) = -\frac{\gamma^{**}\mu(1-m_q)}{Q}$$

at $\gamma = \gamma^{**}$, and

$$c = \frac{(e^{-i\theta_0} - G_{11})^2}{(1-\delta)G_{11}G_{12} + (e^{-i\theta_0} - G_{11})^2}$$

The symmetric multilinear vector functions $B(x,y)$ and $C(x,y,z)$ of $x,y,z \in \mathbb{R}^4$, defined by the Tarlor expansion of (B.1) at the equilibrium, are

$$\begin{aligned}
B_1(x,y) &= \frac{\partial^2 p'}{\partial p \partial v}\Sigma_{ij\in(1,3)}x_i y_j + \frac{\partial^2 p'}{\partial p \partial m}\Sigma_{ij\in(1,4)}x_i y_j + \frac{\partial^2 p'}{\partial u \partial v}\Sigma_{ij\in(2,3)}x_i y_j + \frac{\partial^2 p'}{\partial u \partial m}\Sigma_{ij\in(2,4)}x_i y_j \\
B_2(x,y) &= \frac{\partial^2 u'}{\partial p \partial v}\Sigma_{ij\in(1,3)}x_i y_j + \frac{\partial^2 u'}{\partial p \partial m}\Sigma_{ij\in(1,4)}x_i y_j + \frac{\partial^2 u'}{\partial u \partial v}\Sigma_{ij\in(2,3)}x_i y_j + \frac{\partial^2 u'}{\partial u \partial m}\Sigma_{ij\in(2,4)}x_i y_j \\
B_3(x,y) &= \frac{\partial^2 v'}{\partial p \partial p}x_1 y_1 + \frac{\partial^2 v'}{\partial p \partial u}\Sigma_{ij\in(1,2)}x_i y_j + \frac{\partial^2 v'}{\partial u \partial u}x_2 y_2 \\
B_4(x,y) &= \frac{\partial^2 m'}{\partial p \partial p}x_1 y_1 + \frac{\partial^2 m'}{\partial p \partial u}\Sigma_{ij\in(1,2)}x_i y_j + \frac{\partial^2 m'}{\partial u \partial u}x_2 y_2
\end{aligned} \tag{B.7}$$

and

$$\begin{aligned}
C_1(x,y,z) &= \frac{\partial^3 p'}{\partial p \partial v \partial v}\Sigma_{ijk\in(1,3,3)}x_i y_j z_k + \frac{\partial^3 p'}{\partial p \partial v \partial m}\Sigma_{ijk\in(1,3,4)}x_i y_j z_k \\
&\quad + \frac{\partial^3 p'}{\partial u \partial v \partial v}\Sigma_{ijk\in(2,3,3)}x_i y_j z_k + \frac{\partial^3 p'}{\partial u \partial v \partial m}\Sigma_{ijk\in(2,3,4)}x_i y_j z_k \\
C_2(x,y,z) &= \frac{\partial^3 u'}{\partial p \partial v \partial v}\Sigma_{ijk\in(1,3,3)}x_i y_j z_k + \frac{\partial^3 u'}{\partial p \partial v \partial m}\Sigma_{ijk\in(1,3,4)}x_i y_j z_k \\
&\quad + \frac{\partial^3 u'}{\partial u \partial v \partial v}\Sigma_{ijk\in(2,3,3)}x_i y_j z_k + \frac{\partial^3 u'}{\partial u \partial v \partial m}\Sigma_{ijk\in(2,3,4)}x_i y_j z_k \\
C_3(x,y,z) &= \frac{\partial^3 v'}{\partial p \partial p \partial v}\Sigma_{ijk\in(1,1,3)}x_i y_j z_k + \frac{\partial^3 v'}{\partial p \partial p \partial m}\Sigma_{ijk\in(1,1,4)}x_i y_j z_k \\
&\quad + \frac{\partial^3 v'}{\partial p \partial u \partial v}\Sigma_{ijk\in(1,2,3)}x_i y_j z_k + \frac{\partial^3 v'}{\partial p \partial u \partial m}\Sigma_{ijk\in(1,2,4)}x_i y_j z_k \\
&\quad + \frac{\partial^3 v'}{\partial u \partial u \partial v}\Sigma_{ijk\in(2,2,3)}x_i y_j z_k + \frac{\partial^3 v'}{\partial u \partial u \partial m}\Sigma_{ijk\in(2,2,4)}x_i y_j z_k \\
C_4(x,y,z) &= \frac{\partial^3 m'}{\partial p \partial p \partial v}\Sigma_{ijk\in(1,1,3)}x_i y_j z_k + \frac{\partial^3 m'}{\partial p \partial p \partial m}\Sigma_{ijk\in(1,1,4)}x_i y_j z_k \\
&\quad + \frac{\partial^3 m'}{\partial p \partial u \partial v}\Sigma_{ijk\in(1,2,3)}x_i y_j z_k + \frac{\partial^3 m'}{\partial p \partial u \partial m}\Sigma_{ijk\in(1,2,4)}x_i y_j z_k \\
&\quad + \frac{\partial^3 m'}{\partial u \partial u \partial v}\Sigma_{ijk\in(2,2,3)}x_i y_j z_k + \frac{\partial^3 m'}{\partial u \partial u \partial m}\Sigma_{ijk\in(2,2,4)}x_i y_j z_k
\end{aligned} \tag{B.8}$$

All the possible second and third order partial derivatives of p', u', v' and m', which are nonzero at the equilibrium, are given by

$$
\begin{aligned}
&\frac{\partial^2 p'}{\partial p \partial v} = -\frac{b\mu(1-m_q)(\gamma+1-R)}{Q(1+r^2)},\ \frac{\partial^2 p'}{\partial p \partial m} = \frac{\mu(1-n_0)}{Q}[\rho(\alpha-R)-(\gamma_1-R)]\\
&\frac{\partial^2 p'}{\partial u \partial v} = \frac{b\mu\gamma(1-m_q)}{Q(1+r^2)},\ \frac{\partial^2 p'}{\partial u \partial m} = \frac{\mu\gamma(1-n_0)}{Q}\\
&\frac{\partial^2 u'}{\partial p \partial v} = (1-\delta)\frac{\partial^2 p'}{\partial p \partial v},\ \frac{\partial^2 u'}{\partial p \partial m} = (1-\delta)\frac{\partial^2 p'}{\partial p \partial m},\\
&\frac{\partial^2 u'}{\partial u \partial v} = (1-\delta)\frac{\partial^2 p'}{\partial u \partial v},\ \frac{\partial^2 u'}{\partial u \partial m} = (1-\delta)\frac{\partial^2 p'}{\partial u \partial m},\\
&\frac{\partial^2 v'}{\partial p^2} = \frac{2(1-\delta)}{\delta},\ \frac{\partial^2 v'}{\partial p \partial u} = -2(1-\delta)\left(1+\frac{\gamma\mu(1-m_q)}{Q}\right),\\
&\frac{\partial^2 v'}{\partial u^2} = 2\delta(1-\delta)\left[1+\frac{\gamma\mu(1-m_q)}{Q}\right]^2,\\
&\frac{\partial^2 m'}{\partial p^2} = \frac{2\beta}{Q}(1-\bar{m}^2)(\frac{1}{\delta}-R)[\rho(\alpha-R)-(\gamma+1-R)],\\
&\frac{\partial^2 m'}{\partial p \partial u} = \frac{\gamma\beta}{Q}(1-\bar{m}^2)\left\{(\frac{1}{\delta}-R)-\mu(1-m_q)[\rho(\alpha-R)-(\gamma+1-R)]\right\},\\
&\frac{\partial^2 m'}{\partial u^2} = -2(1-\bar{m}^2)\frac{\mu\beta\gamma^2(1-m_q)}{Q^2}
\end{aligned}
\tag{B.9}
$$

and

$$
\begin{aligned}
\frac{\partial^3 p'}{\partial p \partial v^2} &= \frac{2b^2\mu(1-m_q)(\gamma+1-R)}{Q(1+r^2)^2}, \ \frac{\partial^3 p'}{\partial p \partial v \partial m} = \frac{b\mu(1-n_0)(\gamma+1-R)}{Q(1+r^2)} \\
\frac{\partial^3 p'}{\partial u \partial v^2} &= -\frac{2b^2\gamma\mu(1-m_q)}{Q(1+r^2)^2}, \ \frac{\partial^3 p'}{\partial u \partial v \partial m} = -\frac{b\mu\gamma(1-n_0)}{Q(1+r^2)} \\
\frac{\partial^3 u'}{\partial p \partial v^2} &= (1-\delta)\frac{\partial^3 p'}{\partial p \partial v^2}, \ \frac{\partial^3 u'}{\partial p \partial v \partial m} = (1-\delta)\frac{\partial^3 p'}{\partial p \partial v \partial m}, \\
\frac{\partial^3 u'}{\partial u \partial v^2} &= (1-\delta)\frac{\partial^3 p'}{\partial u \partial v^2}, \ \frac{\partial^3 u'}{\partial u \partial v \partial m} = (1-\delta)\frac{\partial^3 p'}{\partial u \partial v \partial m}, \\
\frac{\partial^3 v'}{\partial p^2 \partial v} &= -\frac{4b\mu(1-\delta)(1-m_q)(\gamma+1-R)}{Q(1+r^2)}, \\
\frac{\partial^3 v'}{\partial p^2 \partial m} &= \frac{4\mu(1-\delta)(1-n_0)}{Q}[\rho(\alpha-R)-(\gamma+1-R)], \\
\frac{\partial^3 v'}{\partial p \partial u \partial v} &= \frac{2b\mu\delta(1-\delta)(1-m_q)}{Q(1+r^2)}\left[\frac{\gamma}{\delta}+(\gamma+1-R)\left(1+\frac{\gamma\mu(1-m_q)}{Q}\right)\right], \\
\frac{\partial^3 v'}{\partial p \partial u \partial m} &= \frac{2\mu\delta(1-\delta)(1-n_0)}{Q}\left[\frac{\gamma}{\delta}-[\rho(\alpha-R)-(\gamma+1-R)]\left(1+\frac{\gamma\mu(1-m_q)}{Q}\right)\right], \\
\frac{\partial^3 v'}{\partial u^2 \partial v} &= -\frac{4b\gamma\delta\mu(1-\delta)(1-m_q)}{Q(1+r^2)}\left(1+\frac{\gamma\mu(1-m_q)}{Q}\right), \\
\frac{\partial^3 v'}{\partial u^2 \partial m} &= -\frac{4\gamma\delta\mu(1-\delta)(1-n_0)}{Q}\left(1+\frac{\gamma\mu(1-m_q)}{Q}\right), \\
\frac{\partial^3 m'}{\partial p^2 \partial v} &= \frac{2b\beta(1-\bar{m}^2)(\gamma+1-R)}{Q(1+r^2)}\left\{(\frac{1}{\delta}-R)-\frac{\mu(1-m_q)}{Q}[\rho(\alpha-R)-(\gamma+1-R)]\right\}, \\
\frac{\partial^3 m'}{\partial p^2 \partial m} &= \frac{2\beta\mu(1-\bar{m}^2)(1-n_0)}{Q^2}[\rho(\alpha-R)-(\gamma+1-R)]^2, \\
\frac{\partial^3 m'}{\partial p \partial u \partial v} &= \frac{b\gamma\beta(1-\bar{m}^2)}{Q(1+r^2)}\left\{-\frac{\mu(1-m_q)(\gamma+1-R)}{Q}-(\frac{1}{\delta}-R)\right. \\
&\quad \left.+\frac{\mu(1-m_q)}{Q}[\rho(\alpha-R)-2(\gamma+1-R)]\right\}, \\
\frac{\partial^3 m'}{\partial p \partial u \partial m} &= \frac{2\mu\beta\gamma(1-\bar{m}^2)(1-n_0)}{Q^2}\left[\rho(\alpha-R)-(\gamma+1-R)\right], \\
\frac{\partial^3 m'}{\partial u^2 \partial v} &= \frac{4b\gamma^2\beta\mu(1-\bar{m}^2)(1-m_q)}{Q^2(1+r^2)}, \\
\frac{\partial^3 m'}{\partial u^2 \partial m} &= \frac{2\gamma^2\beta\mu(1-\bar{m}^2)(1-n_0)}{Q^2},
\end{aligned}
\tag{B.10}
$$

Then the first Lyapunov coefficient can be obtained according to the following formula

$$\begin{aligned} a_2(0) = \frac{1}{2}\mathrm{Re}\left\{e^{-i\theta_0}[< p, C(q,q,\bar{q}) > +2 < p, B(q,(I-J)^{-1}B(q,\bar{q})) > \right. \\ \left. + < p, B(\bar{q},(e^{2i\theta_0}I-J)^{-1}B(q,q)) >]\right\} \end{aligned} \tag{B.11}$$

where p, q, B and C are defined by (B.6), (B.7), (B.8) and I is a 4×4 identity matrix.

References

Agliari, A., Hommes, C. and Pecora, N. (2015), 'Path dependent coordination of expectations in asset pricing experiments: a behavioral explanation', *working paper*.

Alfarano, S., Lux, T. and Wagner, F. (2005), 'Estimation of agent-based models: The case of an asymmetric herding model', *Computational Economics* **26**, 19–49.

Bollerslev, T. (1986), 'Generalized autoregressive conditional heteroskedasticity', *Journal of Econometrics* **31**, 307–327.

Brock, W. and Hommes, C. (1997), 'A rational route to randomness', *Econometrica* **65**, 1059–1095.

Brock, W. and Hommes, C. (1998), 'Heterogeneous beliefs and routes to chaos in a simple asset pricing model', *Journal of Economic Dynamics and Control* **22**, 1235–1274.

Chiarella, C., Dieci, R. and He, X. (2009), *Heterogeneity, Market Mechanisms and Asset Price Dynamics*, Elsevier, pp. 277–344. in *Handbook of Financial Markets: Dynamics and Evolution*, Eds. Hens, T. and K.R. Schenk-Hoppe.

Chiarella, C. and He, X. (2002), 'Heterogeneous beliefs, risk and learning in a simple asset pricing model', *Computational Economics* **19**, 95–132.

Chiarella, C. and He, X. (2003), 'Heterogeneous beliefs, risk and learning in a simple asset pricing model with a market maker', *Macroeconomic Dynamics* **7**, 503–536.

Chiarella, C., He, X. and Hommes, C. (2006), 'A dynamic analysis of moving average rules', *Journal of Economic Dynamics and Control* **30**, 1729–1753.

Di Guilmi, C., He, X. and Li, K. (2014), 'Herding, trend chasing, and market volatility', *Journal of Economic Dynamics and Control* **48**, 349–373.

Dieci, R., Foroni, I., Gardini, L. and He, X. (2006), 'Market mood, adaptive beliefs and asset price dynamics', *Chaos, Solitons and Fractals* **29**, 520–534.

Engle, R. (1982), 'Autoregressive conditional heteroscedasticity with estimates of the variance of UK inflation', *Econometrica* **50**, 987–1008.

Farmer, J. and Joshi, S. (2002), 'The price dynamics of common trading strategies', *Journal of Economic Behavior and Organization* **49**, 149–171.

Gaunersdorfer, A. and Hommes, C. (2007), *A Nonlinear Structural Model for Volatility Clustering*, Springer, Berlin/Heidelberge, pp. 265–288. in *Long Memory in Economics*, Eds. Teyssiere, G. and A. Kirman.

Gaunersdorfer, A., Hommes, C. and Wagener, F. (2008), 'Bifurcation routes to volatility clustering under evolutionary learning', *Journal of Economic Behavior and Organization* **67**, 27–47.

He, X. and Li, K. (2012), 'Heterogeneous beliefs and adaptive behaviour in a continuous-time asset price model', *Journal of Economic Dynamics and Control* **36**, 973–987.

He, X. and Li, K. (2015*a*), 'Profitability of time series momentum', *Journal of Banking and Finance* **53**, 140–157.

He, X., Li, K., Wei, J. and Zheng, M. (2009), 'Market stability switches in a continuous-time financial market with heterogeneous beliefs', *Economic Modelling* **26**, 1432–1442.

He, X. and Li, Y. (2007), 'Power law behaviour, heterogeneity, and trend chasing', *Journal of Economic Dynamics and Control* **31**, 3396–3426.

He, X. and Li, Y. (2015*b*), 'Testing of a market fraction model and power-law behaviour in the DAX 30', *Journal of Empirical Finance* **31**, 1–17.

He, X. and Li, Y. (2015c), 'The adaptiveness in stock markets: testing the stylized facts in the DAX 30', *Working paper, UTS Business School, University of Technology Sydney*.

Hommes, C. (2006), *Heterogeneous Agent Models in Economics and Finance*, Vol. 2 of *Handbook of Computational Economics*, North-Holland, pp. 1109–1186. in *Agent-based Computational Economics*, Eds. Tesfatsion, L. and K.L. Judd.

Hommes, C., Sonnemans, J., Tuinstra, J. and van de Velden, H. (2005), 'Coordination of expectations in asset pricing experiments', *The Review of Financial Studies* **18**, 1955–980.

Kuznetsov, Y. (2004), *Elements of Applied Bifurcation Theory*, SV, New York.

LeBaron, B. (2006), *Agent-based Computational Finance*, Vol. 2 of *Handbook of Computational Economics*, North-Holland, pp. 1187–1233. in *Agent-based Computational Economics*, Eds. Tesfatsion, L. and K.L. Judd.

Li, K. (2014), Asset Price Dynamics with Heterogeneous Beliefs and Time Delays, PhD thesis, University of Technology, Sydney.

Lux, T. (2009), *Stochastic Behavioural Asset Pricing and Stylized Facts*, Elsevier, pp. 161–215. in *Handbook of Financial Markets: Dynamics and Evolution*, Eds. Hens, T. and K.R. Schenk-Hoppé.

Mandelbrot, B. (1963), 'The variation of certain speculative prices', *Journal of Business* **36**, 394–419.

Westerhoff, F. (2004), 'Multiasset market dynamics', *Macroeconomic Dynamics* **8**, 591–616.